Thesis for the Master of Science Degree in Molecular Biosciences

The role of ERM proteins in binding and intracellular transport of Shiga toxin

Audun Sverre Myrset Kvalvaag

CENTRE FOR CANCER BIOMEDICINE

Oslo University Hospital

Department of Molecular Biosciences

The faculty of Mathematics and Natural Sciences

UNIVERSITY OF OSLO

February 2011

"If you're not part of the solution, you're part of the precipitate."

Henry J. Tillman

Acknowledgement

The present work was carried out from January 2010 to February 2011 in the group of Professor Kirsten Sandvig at the Department of Biochemistry, Institute for Cancer Research at the Norwegian Radium Hospital.

I would like to thank my supervisor Kirsten Sandvig for her guidance and expertise, as well as for her warm and welcoming ways. I would also like to express my gratitude to her for giving me the chance to work in a very interesting field in an exceptionally inspirational and professional group.

I would like to thank my supervisor Sascha Pust for teaching me most of what I now know about doing research, as well as for always being there for me. I would also like to thank him for being very clear on what to do and what not to do around the lab.

All the people at the Department of Biochemistry have provided a great working environment and I am grateful to each and every one of you for all your help and support. I would especially like to thank my office mate Ieva Ailte for her contagious energy and good mood, as well as for always keeping the air in the office fresh.

Last but not least, I would like to thank my mother for inspiring me to choose this line of work, as well as for acting as my third supervisor. I would also like to thank my mother, my father and my grandmother for their economical, genetic and moral support, all of which have been essential during this time of my life.

Table of contents

Abstract

In addition to providing morphological support, the actin cytoskeleton is involved in cell motility, endocytosis and intracellular transport. Cytoskeletal interaction with the membrane is an essential part of these processes and is mediated by accesory proteins. The ERM proteins ezrin, radixin and moesin are known to act as linker proteins, connecting the actin cytoskeleton to membrane components such as phosphatidylinositol 4,5-bisphosphate and CD44. The different ERM proteins probably share overlapping functions, but are expressed in a tissue and developmental specific manner. In cultured HeLa cells, mainly ezrin and moesin are reported to be present. To study the role of the ERM proteins in endocytosis and intracellular transport, we treated the cells with siRNA against ezrin and moesin. We then investigated the effect of the knockdown on the binding and retrograde transport of the Shiga toxin (Stx) from the cell exterior, via endosomes, the Golgi apparatus and the endoplasmic reticulum to the cytosol. By siRNA knockdown of ezrin and/or moesin in these cells, we show a decrease in the binding of Stx to the cell surface as well as a decrease in the level of the Stx receptor Gb3 at the plasma membrane. We also show an even larger decrease in the amount of Stx transported from the plasma membrane to the Golgi apparatus and the ER.

Abbreviations

AP-2	Adaptor protein 2
BSA	Bovine Serum Albumin
CDE	Clathrin-dependent endocytosis
CIE	Clathrin-independent endocytosis
CLIC	Clathrin-independent carriers
Complete DMEM	DMEM supplemented with serum, penicillin/streptomycin and glutamine
COPI	Coat protein I
DMEM	Dulbecco's Modified Eagle's Medium
dsRNA	Double stranded RNA
DTT	Dithiothreitol
EBP50	ERM binding phosphoprotein of 50 kDa
EE	Early endosome
ER	Endoplasmic reticulum
ERAD	Endoplasmic Reticulum Associated Protein Degradation
ERC	Endocytic recycling compartment
ERM	Ezrin-radixin-moesin
FBS	Fetal Bovine Serum
FERM	Four point one, ezrin-radixin-moesin
Gb3	Globotriaocylceramide
GEEC	GPI-AP enriched early endosomal compartment
Hepes	(4-(2-Hydroxyethyl)-1-piperazineethanesulfonic acid
HRP	Horseradish peroxidase
ICAM	Intracellular adhesion molecule
Incomplete DMEM	DMEM without serum, penicillin/streptomycin or glutamine
LE	Late endosomes
L-MEM	Leucine free medium
MBV	Multivesicular body
MEM	Minimum Essential Medium w/Earles salts, w/l-glutamine, w/o $NaHCO_3$

MESNa	2-mercaptoethanesulfonic acid sodium salt
mRNA	Messenger RNA
N-ERMAD	N-ERM association domain
PBS	Phosphate buffered saline
pERM	Phosphorylated ezrin-radixin-moesin
$PI(4,5)P_2$	Phosphatidyl-4,5-bisphosphate
PKC	Protein kinase C
RISC	RNA induced silencing complex
RNA	Ribonucleic acid
RNAi	RNA interference
SDS	Sodium dodecyl sulfate
SDS-PAGE	Sodium dodecyl sulfate polyacrylamide gel electrophoresis
siRNA	Small interfering RNA
SNX	Sorting nexin
Stx	Shiga toxin
StxB	Shiga toxin B-subunit
StxB-sulfglyc	StxB modified with two sulfation sites and three glycosylation sites
StxB-sulf2	StxB modified with two sulfation sites
TCA	Trichloroacetic acid
TGN	*trans*-Golgi network

1. Introduction

1.1 Aim of the study

Various toxins can be modified to facilitate their tracking through different compartments in the cell. They also have a cytotoxic potential, which produces a measurable effect at their target location in cells. These attributes make toxins valuable tools in molecular biology, as they can be used to track retrograde transport pathways from the plasma membrane, through endosomes, the Golgi apparatus, the endoplasmic reticulum (ER) and into the cytosol [1, 2]. In addition, toxins are suitable as vectors for carrying epitopes to be presented as antigens by MHC class I molecules [3], for carrying intact proteins [4] and even for bringing nucleotides into the cytosol and the nucleus of cells [5]. Plant and bacterial toxins are also important to study since they pose a global threat to human health. They are relatively common food and water contaminants [6], as well as potential weapons in bioterrorism [7].

In addition to providing morphological support, the actin cytoskeleton is involved in such cellular events as motility, endocytosis and intracellular transport. Cytoskeletal interaction with the membrane is an essential part of these processes, and various accessory proteins are needed to mediate this interaction. Some of the involved proteins are anchored to the cortical actin cytoskeleton [8]. The ERM proteins ezrin, radixin and moesin are identified as actin linkers, connecting the cytoskeleton to various membrane proteins and lipids [9]. They thereby have a possible role in endocytosis and intracellular transport and a general role in cytoskeleton-membrane communication.

In the present study, the role of the ERM proteins in the binding, endocytosis and intracellular transport of Shiga toxin (Stx) and ricin has been investigated. The influence of ERM proteins on Stx binding to the cell surface as well as on the level of the Stx receptor, the glycolipid Gb3, has been emphasized. Cells from the carcinoma

HeLa cell line are reported to mainly express ezrin and moesin of the ERM protein family and have been used as model cells [10, 11].

1.2 Endocytosis and endosomal sorting

The endocytic mechanisms are essential for the cellular acquisition of nutrients, down-regulation of receptor signalling, pathogenic defence, cell integrity and more. The number of components involved in the endocytic network reflects its complexity and new components are described continuously. The different endocytic mechanisms can be divided into five main categories; phagocytosis, macropinocytosis, clathrin-dependent endocytosis, caveolae-dependent endocytosis and clathrin- and caveolae-independent endocytosis (**Fig. 1**).

1.2.1 Phagocytosis and micropinocytosis

Phagocytosis is a mechanism where a cell ingests large particles such as bacteria and cell debris. Cells capable of phagocytosis are specialized cells termed phagocytes [12]. Macropinocytosis is a process where cells internalize bulk extracellular fluid with all its constituents into large vesicles [13].

1.2.2 Clathrin-dependent endocytosis (CDE)

Several receptor-mediated endocytic mechanisms exist, the most extensively studied being clathrin-dependent endocytosis (CDE). This mechanism involves the assembly of a coat of clathrin proteins at the plasma membrane. The clathrin coat contains adaptor proteins able to interact with transmembrane receptors. Other accessory proteins such as Eps15 and epsin that can bind ubiquitin are also involved. Invagination of a clathrin coated pit is followed by formation of an intracellular vesicle which is pinched off from the plasma membrane by the help of dynamin [14, 15].

1.2.3 Clathrin-independent endosytosis (CIE)

Clathrin-independent endocytosis (CIE) can be subdivided in several mechanisms differing from each other in their requirement for various accessory proteins like dynamin [16]. They are also regulated by several different small GTPases like Cdc42 (CLIC/GEEC type endocytosis), RhoA/Rac1 (IL2Rβ endocytic pathway) or Arf6 [17, 18]. In addition, the flotillin proteins have been implicated in internalization [19], but the dependency of GTPases this pathway is unclear [20]. Caveolin-1 is a membrane interacting protein shown to mediate the assembly of caveolin coated invaginations [21], of which the protein cavin is necessary for structural maintenance [22]. Caveolin dependent endocytosis has proven difficult to investigate, partially because the pathway specific membrane protein caveolin-1 is only exposed in the cytoplasm and difficult to label. A dedicated endosomal compartment (the caveosome) was thought to exist, but was recently discarded as an experimental artefact [23]. Nevertheless, CIE can be induced by e.g. the SV40 virus via cavoelin-1, cholesterol and glycosphingolipid enriched membrane domains known as rafts [24, 25]. However, it should be noted that caveolae are regarded as mainly stable, surface connected structures [26].

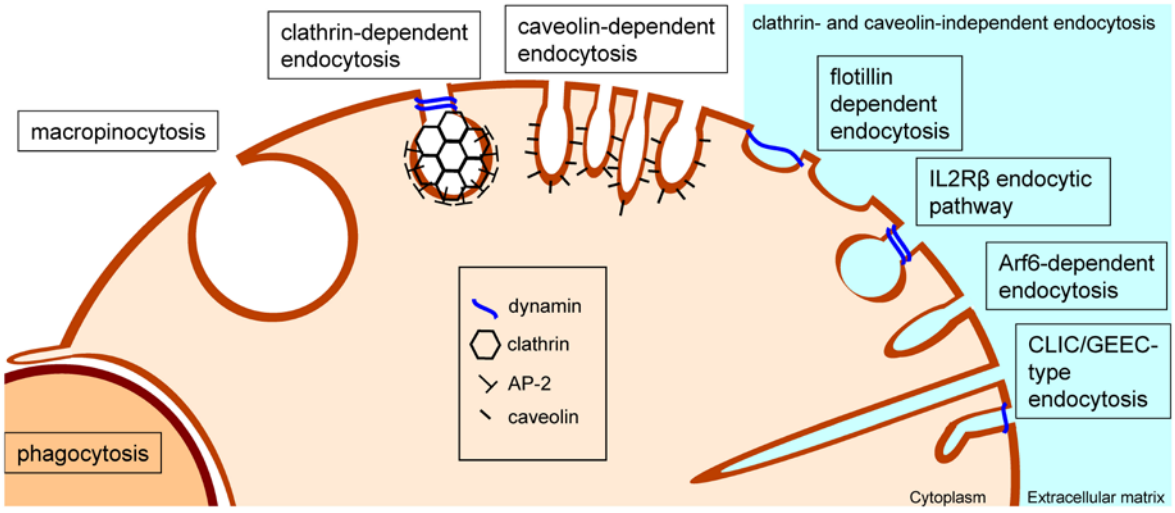

Figure 1 Endocytic pathways. While phagocytosis, macropinosytosis and clathrin dependent endocytosis are widely accepted internalization mechanisms, several other mechanisms have also been shown to play a role in cellular uptake. There is a vast array of proposed accessory proteins accompanying each mechanism, some of the most important ones being illustrated here.

1.2.4 Endosomal sorting

Pathways from CDE and CIE converge in early endosomes (EE), the initial sorting compartment. Several internalized receptors, e.g. the transferrin receptor (TfR) and the low density lipoprotein receptor (LDLR), are normally shuttled back and forth between the cell surface and EE [27-29]. Receptor recycling occurs either by rapid recycling vesicles directly from EE or via the endocytic recycling compartment (ERC). Cargo and receptors that are not recycled, are usually degraded in the low pH of lysosomes [30] (**Fig. 2**). Endosomal sorting enables cells to regulate their sensitivity to extracellular signals by increasing or decreasing the degradation rate of specific receptors [31]. As a consequence of endocytosis, cells internalize large amounts of plasma membrane (PM). Some cells internalize a mass equivalent to their total cell surface several times per hour. Most of the internalized membrane is recycled back to the surface by PM fusion with recycling vesicles, a process enabling cells to maintain a relatively constant size [32].

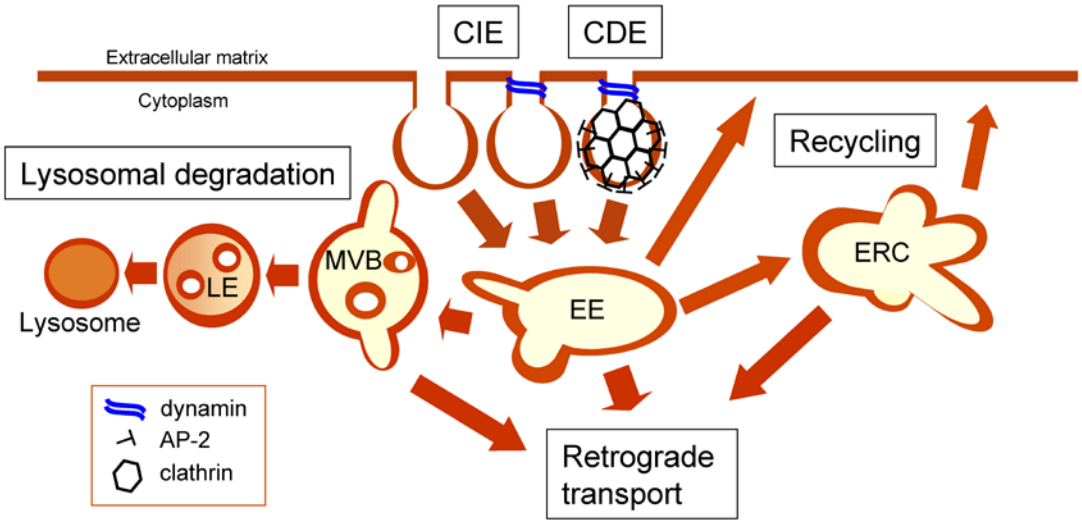

Figure 2 Endosomal trafficking. Clathrin independent (CIE) and clathrin dependent (CDE) pathways converge in early endosomes (EE), the initial sorting station. Cargo is either recycled back to the membrane, degraded in late endosomes (LE) and lysosomes or transported further into the cell by retrograde pathways.

1.2.5 Actin as an endocytic accessory protein

The actin cytoskeleton is composed of actin monomers (G-actin). G-actin exchanges ADP with ATP by interaction with polymerization factors and form actin filaments (F-actin), each monomer adding to the growing end of a filament [33]. The elongation mechanism is utilized in endocytosis by pushing vesicles inwards prior to scission [34]. Actin is also providing the framework for transport of endocytic vesicles [35]. In order to connect actin to the membrane, the ERM proteins are essential players [8].

1.3 Shiga toxin and ricin

1.3.1 Origin

The bacterial toxin Shiga toxin (Stx) is produced by *Shigella dysenteria* and the Stx-like toxins Stx1 and Stx2 (Verotoxin 1 and Verotoxin 2) by *Escherichia coli,* as well as by other bacteria [36]. Their cytotoxic potential is well documented due to numerous occasions of food contamination with severe consequences. Human infection can cause bloody diarrhea with subsequent escalation to haemolytic uremic syndrome (HUS). HUS is a major cause of kidney failure and occasionally death, especially in children [37].

Ricin is a plant toxin which is extracted from the beans of the plant *Ricinius communis.* The beans are mainly used to produce industrial lubricant oil and the toxin can be purified from the waste of this process [38]. Because it needs to be distributed to food or water sources on purpose in order to spread, its main threat to human health is as a weapon in the hands of terrorists. This was exemplified by the assassination of the Bulgarian anti-communist Georgi Makarov in 1978 [7].

1.3.2 Cell association and internalization

Stx is an AB_5 toxin with an A-moiety consisting of the domains A1 and A2 where the enzymatically active A1 domain is activated by release from A2. The A-moiety is non-covalently associated with five B-subunits (**Fig. 3A**). The B-subunits constitute a receptor binding moiety associating with cells by binding up to 15 globotriaocylceramide (Gb3/CD77) glycolipid molecules [39]. Stx can be internalized by CDE and clathrin- and dynamin-independent uptake mechanisms, although the internalization rate is reduced when CDE is inhibited [40].

Ricin is an AB toxin, where the enzymatically active A-subunit is covalently linked to one receptor binding B-subunit through a disulfide bridge (**Fig. 3B**). In contrast to Shiga toxin, the ricin B-subunit binds both glycolipids and glycoproteins with a terminal galactose and is therefore able to be efficiently internalized in most cell types by several different internalization mechanisms [41]. In fact, ricin was used as a tool in one of the first demonstrations of CIE [42].

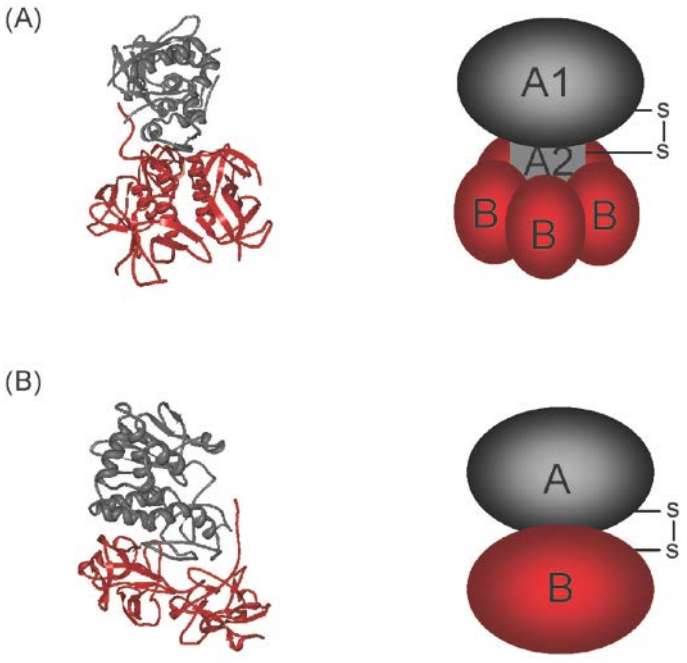

Figure 3 Ribbon structure and structural illustration of Shiga toxin and ricin. (A) Stx (ribbon structure modified from the PDB protein data bank structure 1DM0) consists of an A-moiety of ~32 kDa which is non-covalently linked to a B-moiety composed of five B-subunits of 7.7 kDa each. The A-moiety contains a furin cleavage site, giving rise to the enzymatically active A1 fragment of ~27 kDa and the A2 fragment of ~5 kDa. (B) Ricin (ribbon structure modified from the PDB protein data bank structure 2AAI) consists of an enzymatically active A-subunit covalently linked to a receptor binding B-subunit through a disulfide bridge [36].

1.3.3 Intracellular transport

Upon internalization of Stx and ricin into cells, a proportion of the internalized toxins is transported by retrograde pathways towards the Golgi apparatus [41] (**Fig. 4**). Several differences in the endosome-to-Golgi transport of the two toxins have been demonstrated, e.g. their requirement for clathrin [40] and glycosphingolipids [43], suggesting more than one possible route. The SNX1 and SNX2 components of the retromer complex have been shown to be necessary for the efficient transport of Stx to the Golgi apparatus [44]. SNX8 however, is proposed to inhibit Stx transport but slightly promote ricin transport [45]. Both toxins enter the *trans*-Golgi cisternae and are transported further through the medial- and *cis*- Golgi cisternae. From the Golgi network to the ER, the toxins are thought to be transported in a COPI independent manner because they lack the KDEL sequence necessary for efficient COPI transport [46]. The majority of the internalized toxins are either recycled back to the cell surface, or degraded in lysosomes.

1.3.4 Cytosolic translocation

In order for the A-moiety to exert its cytotoxic effect, the A1 domain in the case of Shiga toxin, and the complete A moiety in the case of ricin, must be transported across the ER membrane and into the cytosol. For Shiga toxin, this process requires that furin creates a nick in a loop formed by the internal disulfide bond between the A1 and A2 domains. The cleavage is likely to occur already in the low pH of the early endosomes [47]. However, furin cleavage alone is not sufficient for the enzyme to translocate, and the rest of the processing probably occurs in the ER. The translocation of both toxins from the ER is thought to be mediated by the endoplasmic reticulum associated protein degradation (ERAD) pathway possibly via the translocon Sec61, in a process requiring the chaperone BiP of the hsp70 family [48]. When in the cytosol, both the Shiga A1 subunit and the ricin A moiety block protein synthesis by removing one adenine residue from an exposed loop on the 28S ribosomal RNA of the 60S subunit [41].

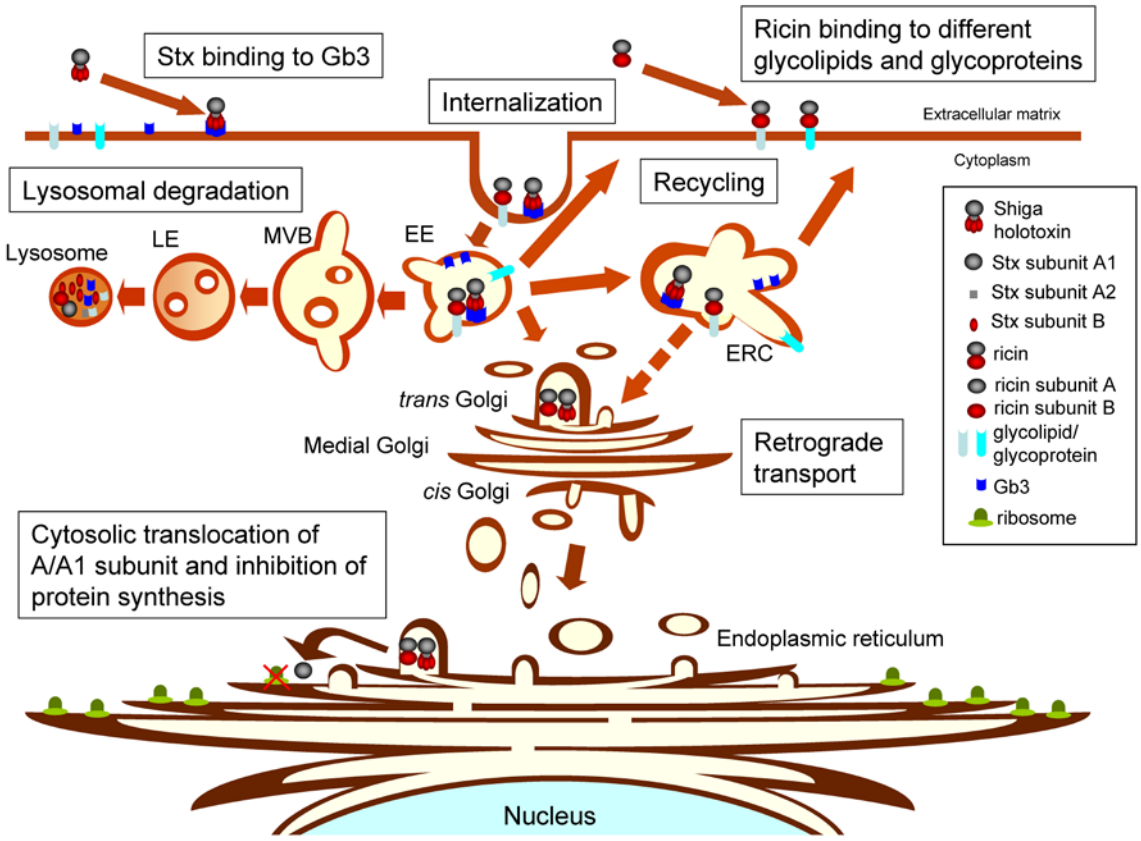

Figure 4 Endocytosis and intracellular transport of Stx and ricin. Most of the toxins are either degraded in lysosomes via multivesicular bodies and late endosomes, or recycled back to the plasma membrane either directly or via the endocytic recycling compartment. A small proportion of the toxins are transported retrogradely to the endoplasmic reticulum. The A/A1 enzymatic subunit is subsequently translocated across the ER membrane to the cytosol. The enzyme then acts by removing one adenine from an exposed loop on the 28S ribosomal RNA of the 60S subunit, thereby inhibiting the protein synthesis.

1.3.5 The Stx receptor Gb3

Stx is known to bind the glycosphingolipid Gb3 (Galα1-4Galβ1-4 Glucosyl ceramide), and to some extent also its derivative globotetraocylceramide (Gb4), prior to endocytosis [49]. Gb3 is present on the cell surface of just a few cell types in healthy tissue, but it is highly expressed in several malignant and metastasizing cells [50]. Gb3 might therefore be a potential target for diagnosis and treatment of certain cancers [51]. The class of Gb3 glycosphingolipids consist of different species, with fatty acid chain lengths ranging from 16 carbon atoms (C16), through C18, C20 and C22 to C24 [52]. Different cell types express different levels of the Gb3 species, with HeLa cells

expressing ~ 50% C24, ~ 20% C22 and ~ 20% C16 [36]. The affinity of Stx varies for the different receptor species, and a simultaneous interaction with different species seems to be most favourable for its internalization. In addition to the Gb3 receptor itself, the surrounding membrane composition is also important for Stx binding [53].

1.4 The ERM proteins and merlin

1.4.1 Structure and orign

The ERM proteins ezrin, radixin and moesin, are a family of proteins found in all metazoan organisms. Together with the proteins four-point-one and merlin the ERM proteins are characterized by a ~300 aa amino-terminus FERM (four point one, ERM) domain also called N-ERMAD (N-terminal ERM association domain). The following ~200 aa domain is enriched in α-helices and culminates in a ~100 aa C-ERMAD (C-terminal ERM association domain) at the carboxy-terminus [54] (**Fig. 5**). All three proteins are present in vertebrates and share some overlapping functions, but they are generally expressed in a developmental and tissue specific manner. Ezrin is primarily expressed in epithelial cells, moesin in endothelial cells [55] and radixin in hepatocytes [56]. Other species only express one ERM protein, so it seems likely that the vertebrate paralogues arose from gene duplication. The N-ERMAD domain on the ERM homologues from species as diverse as sea urchin, *Caenorhabditis elegans, Drosophila melanogaster* and vertebrates show an identity of as much as 74-82% [9].

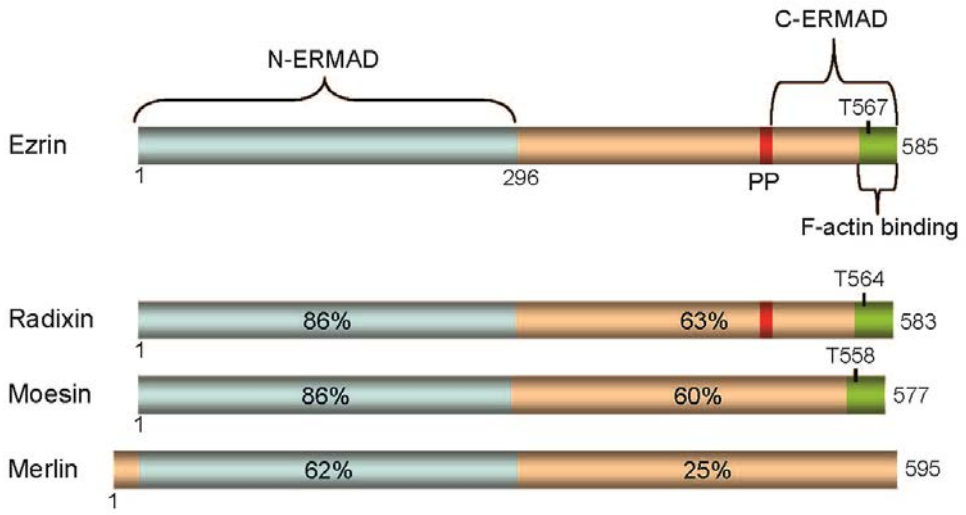

Figure 5 Sequence identity of radixin, moesin and merlin compared to ezrin. (modified from Bretscher et al. [9]). All four proteins can form an intramolecular association between their N-ERMAD/FERM domain and their C-ERMAD, as well as intermolecular associations between each other. ERM members have a carboxy terminal actin association domain (green), while merlin does not. In contrast to moesin, mammalian ezrin and radixin have a proline rich region (PP, red) whose function is unknown. Phosphorylation of the regulatory threonine indicated in the ERM proteins reduces the intramolecular affinity between the two ERMAD domains [9].

1.4.2 Function

The ERM proteins exist either in the cytoplasm in a closed, dormant conformation, or in an open, active conformation at the plasma membrane. They are highly concentrated in actin rich membrane regions such as microvilli and membrane ruffles [57]. The ERM proteins work as a regulated linkage, connecting filamentous actin (F-actin) by the C-ERMAD, to plasma membrane proteins via the N-ERMAD/FERM domain. In the closed conformation, the FERM domain associates with the C-ERMAD and thereby masks at least some protein interaction sites, including the actin binding site [58]. The ERM proteins are also able to hetero- and homo-dimerize and oligomerize in a head to tail fashion, but the functional relevance of this is currently not understood, as contradictory results have been published [59, 60].

Depletion of moesin does not seem to affect mice development [61], while radixin depletion leads to liver failure [62] and ezrin depletion cause mortality after birth [55]. Despite high expression in early thymocytes in mice, isolated ezrin depletion in these cells seem to be tolerated due to redundancy with moesin [63]. These examples suggest that there is a partial overlap in ERM function in some cellular events, but not complete redundancy.

The role of the ERM proteins in endocytosis is still largely elusive, but they have been implicated in recycling of the α1b-adrenergic receptor [64] as well as the β2-adrenergic receptor [65] and in endosomal sorting by association with annexin-II [66]. Additionally, progression of cargo transport through endosomal compartments is mediated by the HOPS (homotypic fusion and protein sorting) complex. Interaction between the HOPS complex and ERM proteins has been shown to be required for delivery of epidermal growth factor receptor (EGFR) to lysosomes [67].

Although the tumour suppressor protein merlin (moesin, ezrin, radixin like protein), the product of the neurofibromatosis (NF2) gene, has a high sequence similarity with the ERM proteins, it is not considered an ERM paralogue and was not studied in this thesis. Mutations in the NF2 gene in humans are known to cause tumours derived from Schwann cells [68] and mice and flies homozygous for mutations in the NF2 gene are not viable [69]. Furthermore, merlin lacks the regulatory threonine conserved in the ERM proteins, as well as an analogue to their actin binding domain.

1.4.3 Regulation of ERM proteins

Phosphorylation of ERM proteins at conserved threonine 567, 558 and 564 residues in ezrin, moesin and radixin, respectively, is found to reduce the affinity of the C-ERMAD for the FERM domain. A two step activation mechanism has been proposed where ERM proteins are recruited to the plasma membrane by phosphatidylinositol 4,5-bisphosphate ($PI(4,5)P_2$) which possibly renders the conserved threonine residue more accessible to phosphorylation [70]. Several vertebrate kinases can phosphorylate the different ERMs at their regulatory Thr, including Rho kinase, Cdc42, protein

kinase Cα (PKCα), PKCθ, NF-κβ-inducing kinase (NIK) and lymphocyte-oriented kinase (LOK) [71-74]. However, from experiments with *Drosophila melanogaster*, novel functions for unactivated moesin have been demonstrated. This indicates that phosphorylation of the regulatory threonine might be redundant in some cellular processes [75].

Additionally, several other phosphorylation sites in the ERM proteins have been proposed, which might mean that the regulatory phosphorylation pattern in these proteins is more complex than initially assumed. The ERM proteins are rapidly tyrosine-phosphorylated following EGF or hepatocyte growth factor (HGF) stimulation [76], and it has been reported that ezrin interacts directly with the HGF receptor MET [77].

Some transmembrane proteins are able to transmit signals either directly, or via non-transmembrane receptors inserted in the outer leaflet of the lipid bilayer. The tetraspanin family of scaffolding proteins is found in all multicellular eukaryotes, and is known to span the plasma membrane four times. By antibody stimulation, the tetraspanin CD81 has been shown to induce phosphorylation of ezrin via the Syk kinase. The phosphorylation leads to F-actin recruitment and cytoskeletal remodelling [78]. The scaffolding protein EBP50 (ERM-binding phosphoprotein of 50 kDa), also known as NHERF1, is considered a possible regulator of microvilli on the surface of epithelial cells. EBP50 contains two PDZ (PSD95/DlgA/zo-1) domains followed by a C-terminal ezrin-binding site, with functional microvilli assembly depending on the presence of one of the PDZ domains as well as the ezrin binding site [79]. EBP50 has also been found in a protein complex residing in lipid rafts, which is functionally dependent of ezrin, suggesting a role for ezrin in raft regulation [80]. Other plasma membrane proteins proposed to serve as docking sites for the ERM proteins include CD44, CD43 and ICAM-2 [81].

1.4.4 The ERM proteins and cancer

Due to their structural similarity, the finding of the tumour suppressor activity of merlin indicated possible roles for the ERM proteins in cancer as well [82]. Some of the most pronounced functions of the ERM proteins are implicated in such cellular events as proliferation, cell-cell and cell-extracellular matrix communication, motility and differentiation, all of which are integral to cancer development [83]. Indeed, several publications have implicated a role for the ERM proteins in cancer, but in contrast to merlin, the ERM proteins are mostly found to be positively correlated to cancer progression [77, 84-86] and tumour metastasis [86-88]. However, moesin has been found to antagonistically regulate Rho pathway activity, where loss of moesin function caused increased migratory cell behaviour [89], an important property of metastatic cells.

2. Materials and methods

2.1 Chemicals

All chemicals had a purity of minimum 98%.

2.2 Cell culture

Different cell lines have different requirements for optimal growth, and growth medium is prepared thereafter, with variations in the basic cell nutrients like salts, amino acids and vitamins. To optimize cell proliferation, the culture medium is often supplemented with blood serum, glutamine and antibiotics. Blood serum contains a large variety of proteins, hormones and electrolytes promoting growth in many cell lines. Glutamine is added as an additional source of reduced carbon, as well as an important precursor in the synthesis of purines, pyrimidines, amino sugars and asparagine and as a component of the citric acid cycle. Antibiotics are added to prevent bacterial contamination. The medium often contains phenol red as a pH indicator as it will change from red at physiological pH 7.4, to orange and yellow in response to a pH decrease and from red to purple in response to a pH increase. The cell cultures are incubated at 37˚C in a carbon dioxide (CO_2) enriched atmosphere providing a buffering system to keep the pH stable.

Trypsin is a serine protease able to cleave peptide chains at the carboxyl ends of lysine and arginine residues except when adjacent to a proline residue. Trypsinization is thereby used to disrupt the cadherins and integrins connecting the cells to each other and to the extracellular matrix, respectively, when passaging them or to reduce the cell confluency. EDTA is able to bind metal ions and enhances the effect of trypsin by starving the medium for Ca^{2+}.

New batches of the human epithelial carcinoma cell lines HeLa (ATCC# CCL-2) were prepared every 4 weeks. The cells were cultured in Dulbecco's Modified Eagle Medium, DMEM (Invitrogen, Life technologies Corp, CA, USA) supplemented with 10% fetal bovine serum (Sigma-Aldrich, MO, USA), 2 mM L-glutamine and 1% penicillin/streptomycin (Invitrogen) in a 5% CO_2 atmosphere at 37˚C. The cells were detached from the wells by trypsinization (0.4 g KCl, 8.0 g NaCl, 1 g glucose, 0.01 g phenol red, 0.5 g trypsin and 0.2 g EDTA in 1 l destilled water) and resuspended in DMEM medium with or without penicillin/streptomycin, depending on the following experiment. The cell number was counted by a Z1 Coulter counter (Beckman Coulter Inc., CA, USA), and cells were seeded out either in Falcon (BD Bioscience, CA, USA) cell culture plates and flasks, or Nunclon (Sigma-Aldrich) cell culture plates.

2.3 RNA interference and transfection

RNA interference (RNAi) is a natural defense mechanism shared by many eukaryote cells. It orchestrates the degradation of foreign RNA molecules introduced by viruses and transposable elements. The presence of double-stranded RNA (dsRNA) attracts a protein called Dicer, a nuclease that cleaves the dsRNA molecule into smaller, doublestranded fragments called small interfering RNAs (siRNA). The siRNAs then assemble into a RNA-induced silencing complex (RISC) along with Argonaute and other proteins. One of the strands of the dsRNA molecule is then cleaved and discarded by Argonaute. The strand remaining bound to RISC directs the complex back to complementary RNA strands, and Argonaute acts again to cleave the strands upon binding.

siRNA transfection is the introduction of specific dsRNA molecules into eukaryote cells, whose given nucleotide sequence matches part of a gene to silence. The RNA interference mechanism is then manipulated to knock down mRNA transcribed from the gene to be silenced, and the function of the protein product is revealed by its absence.

Transient siRNA transfections were performed on HeLa cells to specifically knock down the ERM proteins ezrin and moesin. Cells were incubated at 37˚C in 5% CO_2 24 hours before transfection. For ezrin, the transfections were preformed either with a pool of siRNA oligos with target sequences 5'GCGCGGAGCUGUCUAGUGA3', 5'GCGCAAGGAGGAUGAAGUU3', 5'GGAAUCAACUAUUUCGAGA3' and 5'GCUCAAAGAUAAUGCUAUG3' (referred to as ez-1), or a single oligo with target sequence 5'GCGCGGAGCUGUCUAGUGA3' (ez-2). For moesin, the transfections were performed with single oligos with target sequences 5'CGUAUGCUGUCCAGUCUAA3' (mo-1), and 5'GGCUGAAACUCAACAAGAA3' (mo-2) (Thermo Scientific Dharmacon, PA, USA). Transfection was also carried out with a non-target oligo as a negative control (OnTarget plus siRNA control, cat. # D-001810-01-20, Thermo Scientific). A transfection master mix of was prepared according to the protocol supplied by the manufacturer, containing incomplete DMEM, DharmaFECT 1 Transfection reagent (Thermo Scientific) and 25 nM siRNA for single transfections, or 15 nM siRNA for double transfections. The cells were incubated with the master mix at 37˚C in a total of 2 ml incomplete DMEM in a 5% CO_2 atmosphere for 4-6 hours. Afterwards, the master mix was replaced by 5 ml complete DMEM and the cells were allowed to grow for 72 hours. The effect of the transfections on the relevant protein level (knockdown efficiency) was determined by western blotting.

2.4 SDS-PAGE and western blotting

Sodium dodecyl sulfate polyacrylamide gel electrophoresis (SDS-PAGE) is a method used to separate proteins by their electrophoretic mobility, determined by their size. SDS is an anionic detergent with the ability to interact with hydrophobic amino acids in proteins by wrapping around the protein backbone, and stretching it out at ~ 95˚C. The negative charges carried by SDS practically eliminate the influence of the intrinsic charges of the protein, so different proteins become rod like structures with uniformly charge densities. These are separable by their mobility as a linear function

of the logarithm of their molecular weight. Their mobility is measured by loading protein solutions on polyacrylamide gels with given pore sizes and applying a voltage across the gel. The proteins will travel towards the anode end of the gel, the shortest proteins travelling the fastest.

Western blotting is a method used to identify protein bands by using specific antibodies. After the proteins are separated by SDS page, they are exposed to an electric current pulling the proteins out of the gel and onto an adjacent membrane. The membranes are then incubated in a solution containing a primary antibody specific targeting the desired protein. To keep random proteins from binding to the available areas of the membrane and prevent unspecific antibody binding, different blocking techniques can be applied. After the primary antibody has been allowed to bind, the membrane is incubated in a solution containing a secondary antibody, either conjugated to an enzyme or an infrared dye.

3.0×10^4 HeLa cells were transfected as previously described, washed in PBS buffer (1.1 mM NaH_2PO_4 x H_2O, 5.5 mM NaH_2PO_4 x $12H_2O$, 2.9 M NaCl in dH_2O) and lysed in 500 µl/well lysis buffer (100 mM NaCl, 10 mM Na_2HPO_4, 1 mM EDTA, 1% Triton X-100, 60 mM n-octyl-β-D-glucopyranoside (Sigma-Aldrich), 1 tablet complete protease inhibitor (CΦmplete protease inhibitor, Roche AG, Basel, Switzerland) per 20 ml lysisbuffer pH 7.4). The lysates were pipetted up and down several times in each well before they were collected. Then they were incubated at 95˚C for 5 minutes in SDS sample buffer (0.3 M Sigma 7-9, 8% SDS, 0.01% bromphenolblue, 40% glycerol, 0.4 M DTT) before SDS-PAGE (running buffer: 0.1 M Sigma 7-9 Tris base, 0.1 M HEPES, 3.5 mM SDS) on 10%, 12% or 4-20% polyacrylamide gels (Precise protein gels, Thermo Scientific), at 115V for 50-60 minutes. The proteins were transmitted to an Immobilon –P or –FL PVDF membrane (pore size 0.45 µm, Millipore, MA, USA) by semidry blotting for 70 min at 50 mA/gel (Trans-blot SD, semi-dry transfercell, Bio-Rad laboratories, CA, USA) with transfer buffer (0.3 mM Sigma 7-9 Tris base, 0.2 mM Glycine, dH_2O, 15% v/v methanol). The membrane was dried to avoid unspecific binding and incubated with

primary antibodies against total ezrin, moesin, pERM (cat. # 3145, cat. # 3146, cat. # 3149, respectively, Cell Signaling Technologies Inc, MA, USA), moesin (cat. # 610401, BD Transduction Laboratories, CA, USA), Stx (cat. # SLT1 3C10, Toxin Technology, FL, USA), tubulin or actin (cat. # T5326-200UL and cat. # A3853-200UL respectively, Sigma-Aldrich). The antibodies were diluted in 1% BSA in PBS-T (1.1 mM NaH_2PO_4 x $12H_2O$, 2.9 M NaCl, 0.1% v/v Tween-20 in dH_2O) either at 4˚C overnight or at room temperature for 1 hr. Excess antibody was washed off with PBS-T, and the membranes were incubated either with HRP-linked secondary antibodies (Jackson ImmunoResearch, PA, USA) or IRDye infrared linked secondary antibodies (LI-COR Biosciences, NE, USA) diluted as stated by the manufacturer for 45-60 min at room temperature. The membranes were washed again, and detection of protein bands was preformed either with ECL reagent (Amersham ECL plus western blotting detection system, GE Healthcare Bio-Sciences Corp. NJ, USA) and detection of the protein bands with a Molecular Imager Gel Documentation System (Bio-Rad Laboratories Inc. CA, USA) or Odyssey Infrared Imaging System (LI-COR Biosciences, NE, USA). Protein bands were quantified using Quantity One 4.6.5. Basic software (Bio-Rad).

2.5 Sulfation assay

The Golgi apparatus is an intermediate sorting and packaging organelle used by many macromolecules either *en route* from the Endoplasmic reticulum (ER) to the cell periphery, or during retrograde transport from the cell periphery to the ER. It consists of flattened Golgi cisternae and can be functionally divided into three domains distinguished by their characteristic sets of processing enzymes, namely the cis-, medial and trans-Golgi network. One of these enzymes is the tyrosyl sulfotransferase, found in the trans-Golgi network (TGN), which catalyzes the addition of sulfate at protein sulfation sites. This mechanism can be utilized to measure the amount of specific proteins having reached the TGN at certain time points by replacing the sulfate in the growth medium with a radioactive isotope, immunoprecipitating the

protein and measuring its radiation. Specifically, this method was used to measure the effects of siRNA knockdown of ERM proteins on the retrograde transport of the Shiga toxin B-subunit sulf2 construct.

3.0 x 10^4 HeLa cells were transfected as described earlier. A non target siRNA oligo was used as a negative control. The cells were washed 2 times in pre-warmed, sulfate free SMEM medium (10 ml/L MEM Vitamin solution (100x), 20 ml/L MEM amino acids (50x) 10 ml/L MEM Non-essential amino acids solution (Flow laboratories), 100 mM $CaCl_2$-$2H_2O$, 5.4 mM KCL, 1mM $MgCl_2$-6H2O, 16.4 mM NaCl, 26.19 mM $NaHCO_3$, 10.9 mM NaH_2PO_4-H_2O), and incubated with 0.2 mCi/ml $H_2{}^{35}SO_4$ (Montebello diagnostics, Oslo, Norway) in 500 µl SMEM for 3 hours at 37˚C on a vertical shaker. The wells were then supplemented with 0.5-1.0 mg/ml StxB-sulf2 and incubated at 37˚C for 1 hour. The StxB-sulf2 was a kind gift from Dr. Bruno Goud (Curie institute, Paris, France)

After toxin incubation, the cells were placed on ice and washed with cold PBS before lysis in 400 µl cold lysisbuffer (100 mM NaCl, 10 mM Na_2HPO_4, 1 mM EDTA, 1% Triton X-100, 60 mM n-octyl- β-D-glucopyranoside (Sigma-Aldrich), 1 tablet complete protease inhibitor (Roche) per 20 ml lysisbuffer pH 7.4) for 10 minutes on ice. The lysisbuffer was pipetted up and down in the wells 3-4 times and the lysates transferred to eppendorf tubes. To remove the nuclei, the lysates were centrifuged at 6800 g for 10 minutes at 4˚C and the pellet was discarded.

20 µl protein A-sepharose beads (CL-4B, GE healthcare, Bio-Sciences Corp) per well were washed 3 times in PBS, preceding incubation with 1.5 µl StxB antibody in 100 µl PBS for 1 hour at 4˚C on an orbital shaker. Excess antibody was washed off twice with PBS before the protein beads were added to the lysates. The lysates were then incubated rotating overnight at 4˚C and subsequently centrifuged. Total sulfation was measured by precipitating the total protein content by adding 1 ml 5% TCA w/v to the supernatant followed by 5 minutes centrifugation at ~ 20800 g at 4˚C. 300 µl 0.1 M KOH was applied for 1 hour at room temperature in order to dissolve the pellet, and the total sulfation was then measured on a β-counter.

The protein A-sepharose pellets were washed twice in 0.35 Triton X-100 in PBS before they were denatured in 7.5 µl 4x SDS buffer for 5 minutes at 95˚C. The solution was loaded on a 4-20% gradient gel (precise protein gels, Thermo Scientific) and run at 115 V for ~ 50 minutes. The samples were then blotted as earlier described. The ^{35}S was detected by autoradiography with Kodak BioMax MR film (Kodak, NY, USA) or K-screen (Bio-Rad laboratories) and quantified using Quantity One 4.6.5. Basic software (Bio-Rad).

2.6 Mannosylation assay

N-linked protein glycosylation is catalyzed by oligosaccharyl transferases at asparagine residues in the ER. The attached oligosaccharide is composed of mannose residues among other sugars. By exchanging the mannose in the growth medium with the radioactive isotope [^{3}H]mannose, the proteins glycosylated in the ER are radioactively labelled. Various proteins reaching the ER can thereby be quantified by immunoprecipitation and radiation measurements. The Stx B-moiety can be modified with glycosylation sites and hence serve as a marker for retrograde transport to the ER. A Stx B-moiety was modified with two sulfation sites and three glycosylation sites by our group, termed StxB-sulfglyc.

3.0 x 10^4 HeLa cells were transfected as described earlier. The cells were washed twice in pre-warmed, serum- and glucose-free DMEM medium (Invitrogen, Life technologies Corp.) and incubated with 0.1 mCi/ml D-[2-^{3}H(N)] (PerkinElmer, MA, USA) in 500 µl for 3 hours at 37˚C on a vertical shaker. The wells were then supplemented with 10 µl StxB-sulfglyc together with 1 µg/µl of the ER glycosylase inhibitor Swainsonine and incubated at 37˚C for 3 hrs.

Afterwards, the cells were washed with cold PBS and lysed in 400 µl cold lysis buffer (100 mM NaCl, 10 mM Na_2HPO_4, 1 mM EDTA, 1% Triton X-100, 60 mM n-octyl-β-D-glucopyranoside (Sigma-Aldrich), 1 tablet complete protease inhibitor (Roche) per 20 ml lysis buffer pH 7.4) for 10 minutes on ice. In order to release the cells from

the wells, the lysis buffer was pipetted up and down 3-4 times. Then the lysates were transferred to eppendorf tubes and centrifuged at 6800 g for 10 minutes at 4˚C. The pellet was discarded.

20 µl protein A-sepharose beads (CL-4B, GE healthcare, Bio-Sciences Corp) were washed 3 times in PBS and subsequently incubated with 1.5 µl monoclonal IgG StxB antibody in 100 µl PBS per well for 1 hour at 4˚C on an orbital shaker. Excess antibody was washed off twice with PBS before the protein beads were added to the lysates. The lysates were then incubated rotating overnight at 4˚C and subsequently centrifuged. The total protein content was precipitated by adding 1 ml 5% TCA w/v to the supernatant followed by 5 minutes centrifugation at 20800 g at 4˚C. The supernatant was discarded and 300 µl 0.1 M KOH was applied for 1 hour at room temperature in order to dissolve the pellet. The total mannosylation was then measured on a β-counter.

The protein A-sepharose pellets were washed twice in 0.35 Triton X-100 in PBS before they were denatured in 20 µl 2x SDS loading buffer for 5 minutes at 95˚C. The solution was loaded on a 4-20% gradient gel (precise protein gels, Thermo Scientific) and run at 115 V for ~ 50 minutes. The samples were then blotted as earlier described. The ^{3}H was detected by autoradiography with Kodak BioMax MS (Kodak) film together with a Kodak Biomax TranScreen to increase the signal intensities. The intensity of the bands was quantified using Quantity One 4.6.5. Basic software (Bio-Rad).

2.7 Confocal fluorescent microscopy

Confocal microscopy is an optical imaging technique utilizing point illumination and a spatial pinhole. This eliminates out of focus light, thereby increasing the optical resolution and contrast of a micrograph compared to conventional fluorescence microscopy where the entire sample in the optical path is excited. Lasers fire a beam of light of a certain wavelength point by point through the focal plane and when the

light sequentially strikes the molecules of the specimen, electrons are raised to higher, unstable energy levels. When returning to their original energy state, the electrons releases energy as photons with specific wavelengths detectable by the microscope and a computer is then able to build an image from all the detected photons.

3.0 x 10^4 HeLa cells were seeded out on coverslips, followed by transfection as described earlier. Depending on the experiment, they were incubated with e.g. StxB or antibodies for live cell staining in CO_2 incubators, or no pre-treatment. Then the cells were washed 3 times in PBS buffer preceding fixation in a 10% formalin solution (Sigma-Aldrich) or 4% formaldehyde (Sigma-Aldrich) for 18 minutes. The washing step was repeated and, when required, the cells were permeabilized for 2 minutes in 0.2% Triton X-100 in PBS. The washing step was repeated again and the cells were incubated 1 hour in a 10% FBS in PBS blocking solution at room temperature to avoid unspecific binding of antibodies. The cells were then incubated in primary antibody binding ezrin [1:200], moesin [1:200], pERM [1:200], StxB [1:500] (cat. # 3145, cat. # 3146, cat. # 3149, respectively, Cell Signaling) or Gb3 [1:50] (cat. # 551352, BD pharmingen) diluted in blocking solution for 1 hr. After another washing step including an additional 5 min wash in blocking solution, the cells were incubated in Cy2 [1:200] and Cy3 [1:500] labelled secondary antibodies (Jackson Immunoresearch, PA, USA) diluted in blocking solution. The washing step was repeated again including an additional wash in dH2O before the cells were mounted on nuclear staining reagent DAPI (4’6-diamidino-2-phenylindole) diluted in Prolong Gold Molecular Probes (Invitrogen) overnight at 37˚C. The cells were analyzed with a Zeiss LSM duo, Zeiss LSM 710 or Zeiss LSM 780 confocal microscope (Carl Zeiss Inc. Oberkochen, Germany) and pictures of single plane sections were prepared with Zeiss LSM image examiner and labelling was quantified with the freely downloadable software ImageJ.

2.8 Biotin conjugated Shiga toxin endocytosis assay

The Shiga toxin (Stx) is known to be taken up both by clathrin-dependent and clathrin-independent endocytosis. It is possible to quantify endocytosis by conjugating Stx with biotin through a disulfide bridge and allowing internalization of the complex. The compound sodium 2-mercaptoethanesulfonate (MESNa) is non cell permeable and able to specifically disrupt the disulfide bridge of the Stx-biotin complex. By adding MESNa to one of the wells in parallel samples prior to cell lysis, all the extracellular Stx will release its bound biotin. After cell lysis, biotin-Stx is labeled by a TAG® detection label and precipitated by streptavidin coated magnetic beads. The light intensity from electrochemically stimulated ruthenium atoms contained in the TAG label is quantified by a specialized electroluminescent detection instrument. The MESNa treated wells will display the amount of endocytosed biotin-Stx and the untreated wells will display the total biotin-Stx.

3.0×10^4 HeLa cells were transfected for 3 days as earlier described with 2 parallels per siRNA oligo, and then washed in pre-warmed Hepes buffered medium (MEM supplemented with 2 mM L-glutamine, 1% Penicillin Streptomycin and 20 mM Hepes, pH 7.7). Each well was then added 500 µl Hepes buffered medium containing 1:3000 Biotin-Stx (stock concentration 125 µg/ml). The Stx was biotinylated with reducable ImmunoPure NHS-SS-biotin according to the producers protocol (Thermo Scientific). The cells were then allowed to internalize the toxin at 37˚C for 20-30 minutes, before endocytosis was arrested by placing the cells on ice, and unbound toxin was washed off with cold dialysis buffer (2 mM $CaCl_2 \times H_2O$, 20 mM Hepes, 0.1 M NaCl, pH 8.6). One of the parallels with identical conditions was treated with freshly prepared MESNa solution (0.1 M MESNa in 2 mg/ml BSA in dialysisbuffer pH 8.6) 30 minutes on ice, before they were washed twice in 5 ml cold dialysisbuffer and finally lysed 10 minutes in 260 µl lysisbuffer (100 mM NaCl, 10 mM Na_2HPO_4, 1 mM EDTA, 1% Triton X-100, 60 mM n-octyl-β-D-glucopyranoside (Sigma-Aldrich), 1 tablet complete protease inhibitor (Roche) per 20 ml lysisbuffer pH 7.4). The other parallel of each sample was only washed with cold dialysisbuffer and added

lysisbuffer for a total of 40 minutes. 3 replicates of 75 µl from each sample were then transferred to a 96-well plate along with a blank triplicate containing only lysisbuffer, and 40 µl of a solution containing 0.5 µg/ml TAG labeled Stx antibody mixed with 0.1 mg/ml streapavidin coated beads (Dynabeads M-280 streptavidin, Invitrogen, Dynal AS, Oslo, Norway) in assay diluent (0.2% BSA in 0.5% Tween-20 in PBS) was added to each well. The plate was shaken for 90 minutes on a vertical shaker at RT, before 60 µl of assay diluent was added to each well. The amount of TAG labeled Stx coupled to beads through streptavidin-biotin binding was finally analyzed using a M1R analyzer (M-series workbench 2001-2004, BioVeris) and the ratio of internalized Stx was calculated.

2.9 Lipid extraction and high performance thin layer chromatography (HPTLC)

Thin layer chromatography (TLC) is used to separate mixtures of various substances like carbohydrates, lipids and nucleotides. The substances are dissolved in a mobile phase which is passed through a stationary phase. The different substances travel at different rates through the stationary phase due to different affinities for the stationary material and are hence separated during their passage. A foundation of aluminium foil, glass or plastic is covered by an adsorbing, stationary material, such as a silica gel. Lipids running on a silica gel will be separated according to their hydrophobicity determined by their headgroups and hydrocarbon chains, the more hydrophobic lipids travelling the longest. The sample is applied to the stationary phase and incubated with a mobile phase, able to draw the sample up the plate by capillary action. After separation, the substances can be visualized by different mechanisms like chemical staining or antibody detection.

1.2 x 10^6 HeLa cells were seeded in 225 cm^2 Falcon (BD Bioscience) flasks and transfected as previously described. The cells were washed with 10 ml trypsin before they were incubated for 10 min at 37˚C in 5 ml of the same trypsin solution. The trypsinization process was abolished by addition of 5 ml DMEM supplemented with

serum and the detached cells were collected. Afterwards, 400 µl of the cell solution was diluted in 20 ml isoton solution (Coulter Isoton II Diluent, Beckman Coulter Inc.) and counted by a Z1 Coulter counter (Beckman Coulter Inc.). An equal number of cells (~ 1.0 x 10^7 cells) from the different samples was transferred to 13 ml Pyrex tubes pre-cleaned in MeOH and the tubes were mass equilibrated with complete DMEM. The tubes were centrifuged (Sorvall RC 6 plus, Thermo electron corporation) with a SS-34 rotor (Thermo scientific) for 8 min at 400 g at 10˚C. The supernatants were discarded before the pellets were washed in PBS and resuspended in 10 ml MeOH. The samples were then sonicated in a waterbath (Branson 3200) for 10 min and subsequently centrifuged for 10 min at 5500 g at 10˚C. The supernatants were filtered into special 60 ml centrifugation bottles (SampleGenie GeneVac glass tubes, GeneVac inc., NY, USA) and the pellets were resuspended in 10 ml 2:1 MeOH:chloroform before another 10 min sonication and 10 min centrifugation at 5500 g at 10˚C. The sonication, centrifugation and resuspension were repeated two additional times with a resuspension solution of 10 ml 1:1 MeOH:chloroform and 10 ml 1:2 MeOH:chloroform, respectively . Thereafter, the total supernatant solutions of 40 ml were completely evaporated during centrifugation (EZ-2 standard, personal evaporator, GeneVac inc.) set to low Boiling Point mode for ~ 4 hrs. The extracts were resuspended in 5 ml 1 M NaOH and incubated in a water bath at 37˚C for 1 hr to hydrolyse the ester-bonds of phospholipids and triglycerides. The pH was then neutralized by addition of 0.5 ml 10 M HCl before the extracts were transferred to dialysis tubes (Spectra/Por, Spectrum Laboratories, Inc.). To ensure that all the extracts were transferred, the GeneVac tubes were washed with 3 ml water and the water was added to the dialysis tubes. The dialysis tubes were lowered into 5 l destilled water and dialysis was carried out to remove salts and free fatty acids for 48 hrs at 4˚C with water replacement twice a day. The purified glycolipid extracts were transferred to the special GeneVac centrifugation bottles (GeneVac inc.) and the dialysis tubes cleaned out with 5 ml water. Complete evaporation during centrifugation was carried out with a GeneVac personal evaporator (GeneVac inc.) set

to aqueous mode for 9 hrs. The extracts were then redisolved in 250 µl 2:1 chloroform:MeOH and stored at -20˚C.

50 µl of each sample were applied ~ 1 cm above the open end of a 10 x 10 cm silica covered HPTLC plate (MERCK, NJ, USA) by a Linomat5 (CAMAG, Berlin, Germany) sample applier along with 15 µl standard with glycosphingolipids extracted from human erythrocytes (a kind gift from Prof. Dr. Johannes Müthing, Institute for Medical Physics and Biophysics, University of Münster, Germany). The plate was then lowered into a glass-chamber and the chamber closed by a silicone tightened lid. Previously 50 ml chloroform:methanol:water (70:30:4 v/v) had been added to the glass chamber and the fumes had been allowed to equilibrate for > 2 hrs. The glycolipids were drawn up the silica gel until the leading edge of the liquid phase had reached 1 cm below the top of the plate. Afterwards, the plate was soaked in a 0.3% orcinol solution (0.3 g orcinol in 100 ml 3M H_2SO_4 / H_2O) for 20 s before the bands were visualized by heating to 100˚C for ~ 5 min.

2.10 Transfection with siRNA resistant (siRNAr) genes

Amino acids are encoded by a nucleotide triplet in the mRNA. However, most of the amino acids can be encoded by more than one nucleotide triplet. The same protein can thereby be transcribed from genes with different DNA sequences. Silent mutations occur when genes are changed by DNA point mutations while the translated amino acid sequence remains unchanged. Transfection with siRNA oligos induces cellular defence mechanisms targeting mRNAs containing the specific siRNA nucleotide sequence. By re-transfecting cells with a gene encoding a protein that has been knocked down, but with a DNA sequence different from the chromosomal DNA, an mRNA sequence different from the siRNA will be transcribed. The activated defence machinery will not recognize the mRNA and a functional protein will be translated. This method is applied to control that the phenotypical effects of a knockdown is actually caused by a loss-of-function of the relevant protein. If that is the case, the

original phenotype should be restored in response to rescue of the original protein level.

3.5 x 10^4 HeLa cells were seeded in Falcon (BD Bioscience) six well plates and transfected as earlier described, two wells per condition. On the second day of transfection, one of the wells in each condition was transfected again, this time with DNA expression vectors. The control sample was transfected with an empty vector while the moesin and ezrin siRNA treated cells were transfected with vectors carrying moesin and ezrin siRNAr genes, respectively. The mutated moesin and ezrin genes were modified and inserted in a vector by DNA2.0, CA, USA. A transfection master mix was prepared according to the protocol supplied by the FuGENE 6 transfection reagent manufacturer (Roche), containing either 1 μg expression vector / 6 μl FuGENE 6 or 2 μg expression vector / 6 μl FuGENE 6, diluted in 1.994 ml serum free DMEM (Invitrogen, Life technologies Corp.) per condition. The cells were incubated with the master mix at 37˚C in a 5% CO_2 atmosphere and allowed to grow for an additional 24 hrs. The knockdown and rescue levels of the relevant proteins were determined by western blotting.

3. Results

In order to investigate the role of ERM (ezrin, radixin and moesin) proteins in binding and retrograde transport of Shiga toxin (Stx), HeLa cells were treated with small interfering RNA (siRNA) oligos depleting ezrin or moesin. Protein knockdown by treatment with siRNA results from activation of cellular defense mechanisms aimed at degrading the siRNA. Endogenous mRNA containing the same nucleic acid sequence as the siRNA oligo will not be distinguished and also depleted. To control that the phenotypic response was not due to the treatment itself, control cells were treated with non targeting oligos. Reduction of a protein to a certain threshold level might be determined by small differences in siRNA knockdown efficiencies, but result in large differences in the phenotypic effect. Several ERM siRNA oligos were tested and the most efficient ones applied to the following experiments.

3.1 The effect of ERM depletion on transport of Stx to the *trans*-Golgi network (TGN)

Protein sulfation is known to occur at tyrosine residues in the TGN by tyrosylprotein sulfotransferases (TPST). Exchanging the sulfate in the growth medium with radioactive [^{35}S]sulfate thereby causes radioactive labeling of sulfated proteins. The Shiga toxin B (StxB) subunit is known to be endocytosed and transported retrogradely through various cellular compartments, like the Golgi network and the ER. In order to assess the effect of ERM depletion on the retrograde transport of Stx to the TGN, ezrin and moesin knockdown cells were incubated with [^{35}S]sulfate and a modified construct of the StxB subunit (StxB-sulf2). StxB-sulf2 contains two sulfation sites enabling quantitative measurements of labeled StxB. The cells were lysed and StxB was immunoprecipitated from the lysates. To control the activity of the total sulfotransferases in the different samples, the remaining sulfated protein population in the lysates was measured in addition to the amount sulfated StxB. When the ERM protein levels in the siRNA treated cells were reduced below a threshold of ~ 30% for

ezrin and ~ 20% for moesin, there was a decrease in the level of sulfated StxB. As shown in figure 6A, there was a decrease of ~ 70% by knockdown with the ezrin-1 (ez-1) siRNA oligo and a decrease of ~ 90% with the ezrin-2 (ez-2) oligo compared to control. The moesin-1 (mo-1) oligo gave a reduction of ~ 60% and the moesin-2 (mo-2) oligo a reduction of ~ 30%. The sulfated StxB level was reduced to ~ 10% after simultaneous knockdown with the ez-1 and mo-1 oligos as well as with the ez-2 and mo-2 oligos. The total sulfated protein population in the lysates was not significantly affected. Also shown are representative autoradiographs of the ^{35}S radiation intensities from sulfated Stx. Representative blots of the ezrin and moesin levels in ezrin and moesin siRNA treated cells relative to control cells are shown in figure 6B. The ezrin level was reduced to ~ 35% (ez-1), and ~ 15% (ez-2), and the moesin level was reduced to ~ 20% (mo-1) and ~ 25% (mo-2). In summary, there was a significant reduction of Stx transport to the TGN after ERM depletion.

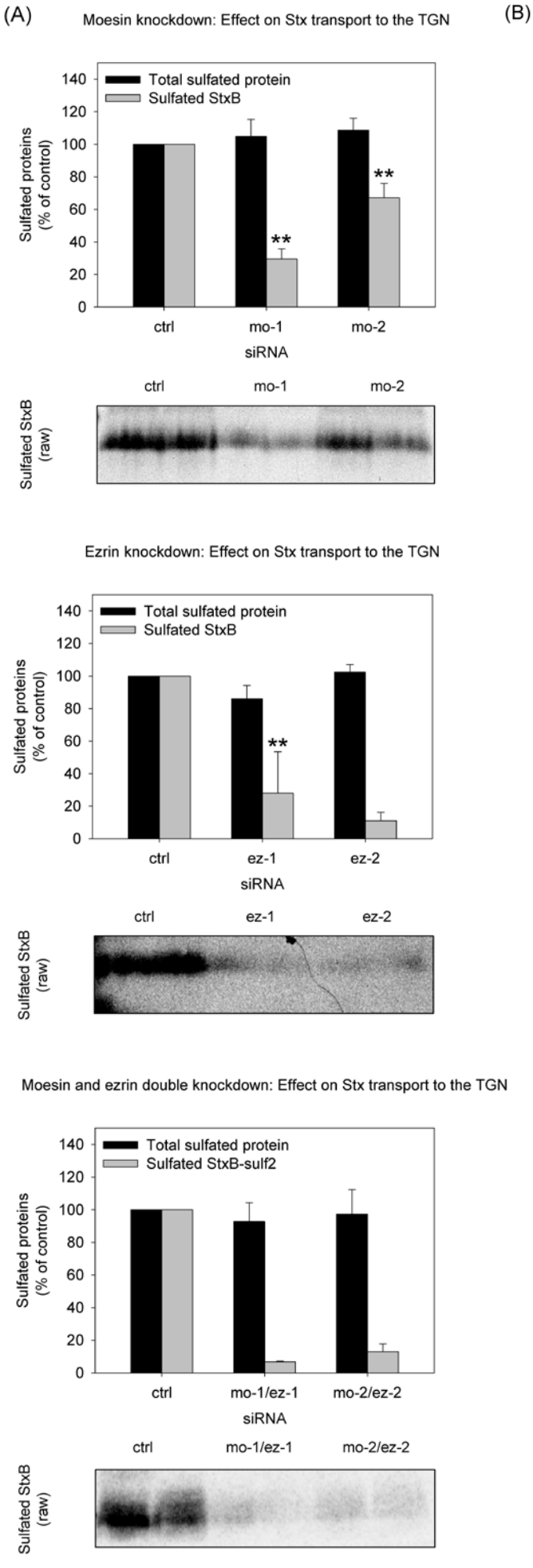

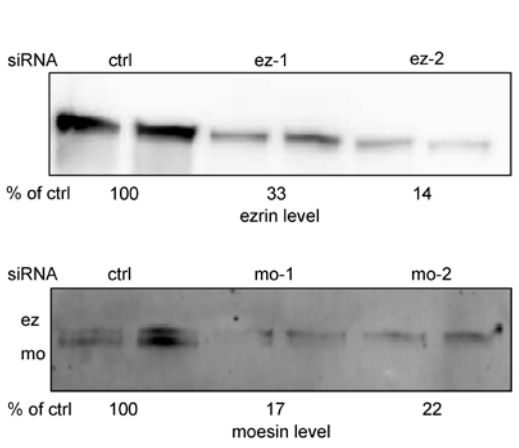

Figure 6 Transport of Stx to the *trans*-Golgi network in ezrin and/or moesin depleted HeLa cells. siRNA treated HeLa cells were incubated with StxB in growth medium supplemented with $^{35}SO_4^{2-}$. (A) Amount of sulfated StxB in control cells compared to knockdown cells, including representative autoradiographs of raw sulfated StxB intensities with two lanes per condition (mean intensity ± S.D., ez-1; n=3, ez-2; n=2, mo-1; n=3, mo-2; n=3, ez-1/mo-2; n=2, ez-2/mo-2; with StxB in n=2. **; $p < 0{,}005$). (B) Representative blots of ezrin and moesin levels in knockdown cells relative to control cells. The proteins were separated by SDS-PAGE and blotted to a PVDF membrane. The ezrin blot was stained with an ezrin specific primary antibody and visualized by HRP-conjugated secondary antibody staining and ECL treatment. The moesin bands were stained with an ERM specific primary antibody but only the level of moesin was quantified (lower band). The bands were visualized by fluorescence.

3.2 ERM knockdown effect on the retrograde transport of ricin

Ricin is able to bind glycolipids and glycoproteins on the cell surface, and can subsequently be endocytosed by several mechanisms. After internalization, ricin is transported retrogradely to the TGN. To study the effect of ERM depletion on retrograde transport in general, ricin transport to the TGN was measured. HeLa cells depleted of ERM proteins were incubated with radioactive [^{35}S]sulfate and a genetically modified ricin construct (ricin-sulf1). Ricin-sulf1 contains a sulfation site, and was therefore labelled in the TGN. The cells were lysed and ricin was immunoprecipitated from the lysates. The radioactivity of the remaining sulfated proteins in the lysates was measured in addition to the amount of sulfated ricin. As shown in figure 7, ERM depletion had no noteworthy effect on retrograde transport of ricin. A representative autoradiogram is also displayed.

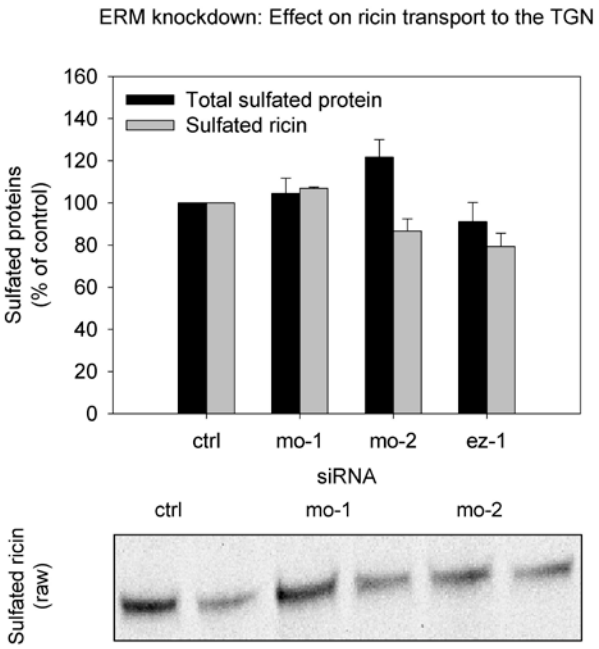

Figure 7 Ricin transport to the TGN in ERM depleted HeLa cells. siRNA treated HeLa cells were incubated with ricin in growth medium supplemented with [^{35}S]sulfate. The amount of sulfated ricin in control cells compared to knockdown cells, included a representative autoradiogram of raw ricin radiation intensity is shown, (n=2).

3.3 The effect of ERM knockdown on the transport of Stx to the endoplasmic reticulum (ER)

To investigate whether Stx transport was reduced further along the retrograde pathway, the amount Stx reaching the ER was measured in ERM depleted HeLa cells.

Protein glycosylation is known to occur at asparagine residues in the ER by oligosaccharyl transferases. The process involves adding a mannose rich oligosaccharide to the proteins. By exchanging the mannose in the growth medium with radioactive [^{3}H]mannose, glycosylated proteins are radioactively labelled. As mentioned earlier, the StxB is known to be transported retrogradely through the ER. In order to assess the effect of ERM depletion on the retrograde transport of StxB to the ER, ezrin and moesin knockdown cells were incubated with [^{3}H]mannose and another StxB construct (StxB-sulfglyc). StxB-sulfglyc contains three glycosylation sites, in addition to the sulfation sites. Similarly as for the StxB-sulf2 construct, radioactive labelling of the StxB-sulfglyc construct enabled quantitative measurements of StxB transported to the ER. The cells were lysed and StxB was immunoprecipitated from the lysates. Both the remaining glycosylated protein population and the precipitated StxB were measured. As shown in figure 8A, there was a decrease in the level of glycosylated StxB of ~ 30% with the ez-1 oligo and ~ 60% with the ez-2 oligo compared to control. With the mo-1 oligo there was a ~ 90% decrease. The figure also shows a representative autoradiography is also displayed. The level of the total glycosylated proteins was not significantly affected. A representative blot of the ezrin and moesin levels in siRNA treated cells relative to control cells is shown in figure 8B. The moesin level was reduced to ~ 5% (mo-1) and the ezrin level was reduced to ~ 25% (ez-2). Similarly to what was demonstrated for the effect on transport to the TGN, there was a significant reduction in transport to the ER.

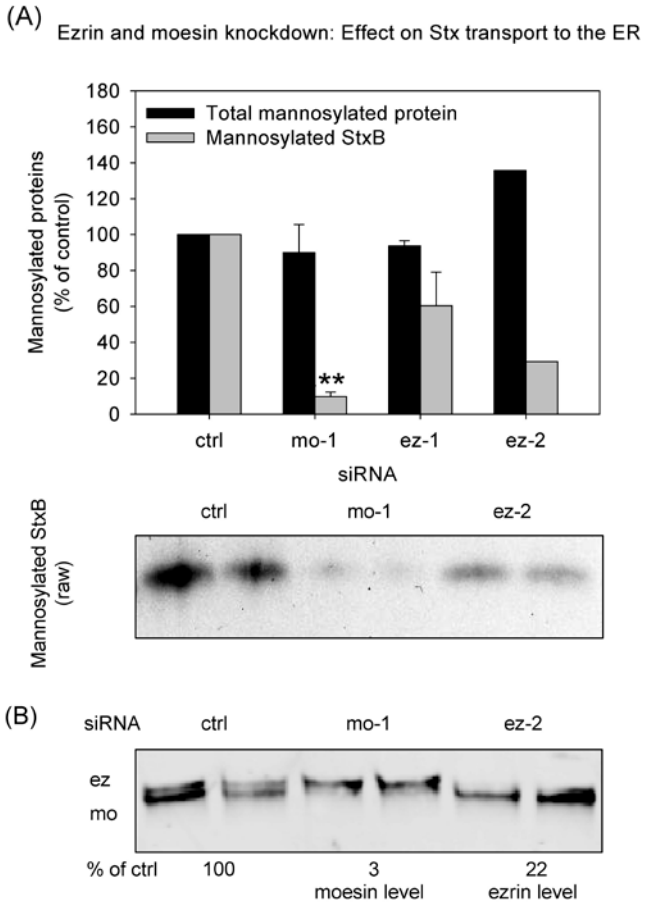

Figure 8 Transport of StxB to the ER in ERM depleted HeLa cells. siRNA treated HeLa cells were incubated with StxB in growth medium supplemented with radioactive [^{3}H]mannose. (A) Amount of total glycosylated proteins and glycosylated StxB in control cells compared to knockdown cells with a representative autoradiogram of raw intensities from one experiment, (mean intensity ± S.D., mo-1; n=3, ez-1; n=2, ez-2; n=1. **; $p < 0{,}005$). (B) Representative blot of ezrin (upper band) and moesin (lower band) levels in knockdown cells relative to control cells. The proteins were separated by SDS-PAGE and blotted to a PVDF membrane. The blot was stained with a primary antibody detecting both ezrin and moesin. The bands were visualized by fluorescence.

3.4 The effect of ERM depletion on binding and endocytosis of Stx

As ERM proteins had a clear effect on Stx transport upstream of the Golgi network, their role in internalization was investigated.

Stx is able to bind the glycosphingolipid Gb3 and can subsequently be endocytosed by different endocytic mechanisms. Stx conjugated to biotin was allowed to bind and enter ERM depleted and control HeLa cells. Sodium 2-mercaptoethanesulfonate (MESNa) releases extracellular biotin, so by comparing MESNa treated and untreated cells, the level of internalized Stx-biotin could be measured. All the cells were lysed and the remaining Stx-biotin conjugates were immunoprecipitated. The biotin was

labelled by an antibody containing ruthenium atoms able to emit light upon electrochemical stimulation. A representative experiment displaying raw data is shown in figure 9A. By comparing the control cells and ERM knockdown cells, no relevant change in the level of endocytosis was found (figure 9B and C). However, the level of total cell associated Stx was decreased to ~ 65% (ez-1) and ~ 45% (mo-1) in ERM depleted cells compared to control (figure 9B). Additionally, the total cell associated Stx was reduced to ~ 50% compared to control, while the level of endocytosis was unchanged in an experiment with simultaneous knockdown of moesin and ezrin (figure 9C). Figure 9D shows representative blots of the ezrin and moesin levels in siRNA treated cells compared to control. The ezrin level was reduced to ~ 5% (ez-1) and the moesin level reduced to ~ 7% (mo-1). The ERM proteins did not seem to be involved in the endocytosis itself, but was clearly important for the association of Stx to the cell surface.

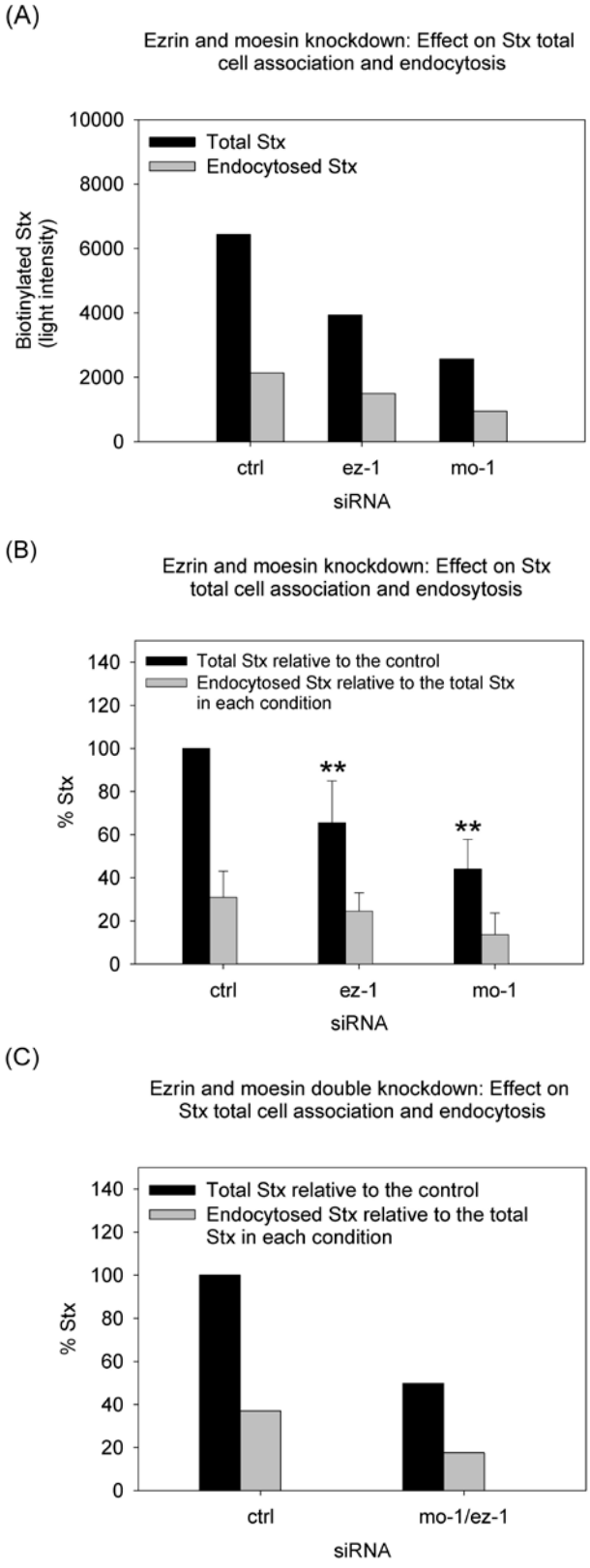

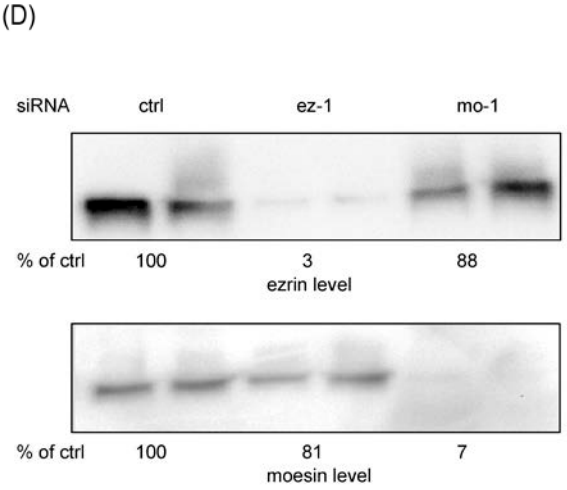

Figure 9 Binding and endocytosis of Stx in ezrin and/or moesin depleted HeLa. siRNA treated HeLa cells were incubated with a Stx-biotin conjugate and the amount of total cell associated and internalized Stx-biotin was quantified. (A) Raw data from one experiment. (B) Quantification of internalized and total cell associated Stx (mean intensity ± S.D., n=5. **; $p < 0{,}005$). The level of Stx endocytosis in knockdown cells relative to the total cell associated Stx in each condition is shown in light gray and total associated Stx in knockdown cells relative to control cells is shown in black. (C) Endocytosed and total associated Stx after simultaneous ez-1 and mo-1 knockdown (details described in B). (D) Representative blots of the ezrin and moesin levels in knockdown cells relative to control cells. The blots were stained with specific ezrin and moesin primary antibodies and visualized by ECL treatment.

3.5 Visualizing the effect of ERM knockdown on the transferrin receptor (TfR)

The transferrin receptor (TfR) is known to be endocytosed by clathrin-dependent endocytosis (CDE). To investigate whether the decrease in total cell-associated Stx in response to ERM depletion was due to a general role of ERM proteins on CME, HeLa cells were treated with siRNA targeting ezrin and moesin. After fixation and permeabilization, cells were stained for ezrin, moesin and TfR. The primary antibody staining was visualized by fluorescent secondary antibody treatment, ezrin and moesin in green and the TfR in red, while the nucleus was stained with DAPI (blue). As shown in figure 10A-D, neither the level nor the distribution of TfR seemed to be affected by ERM depletion compared to control cells, indicating that the process of CME is independent of ERM proteins.

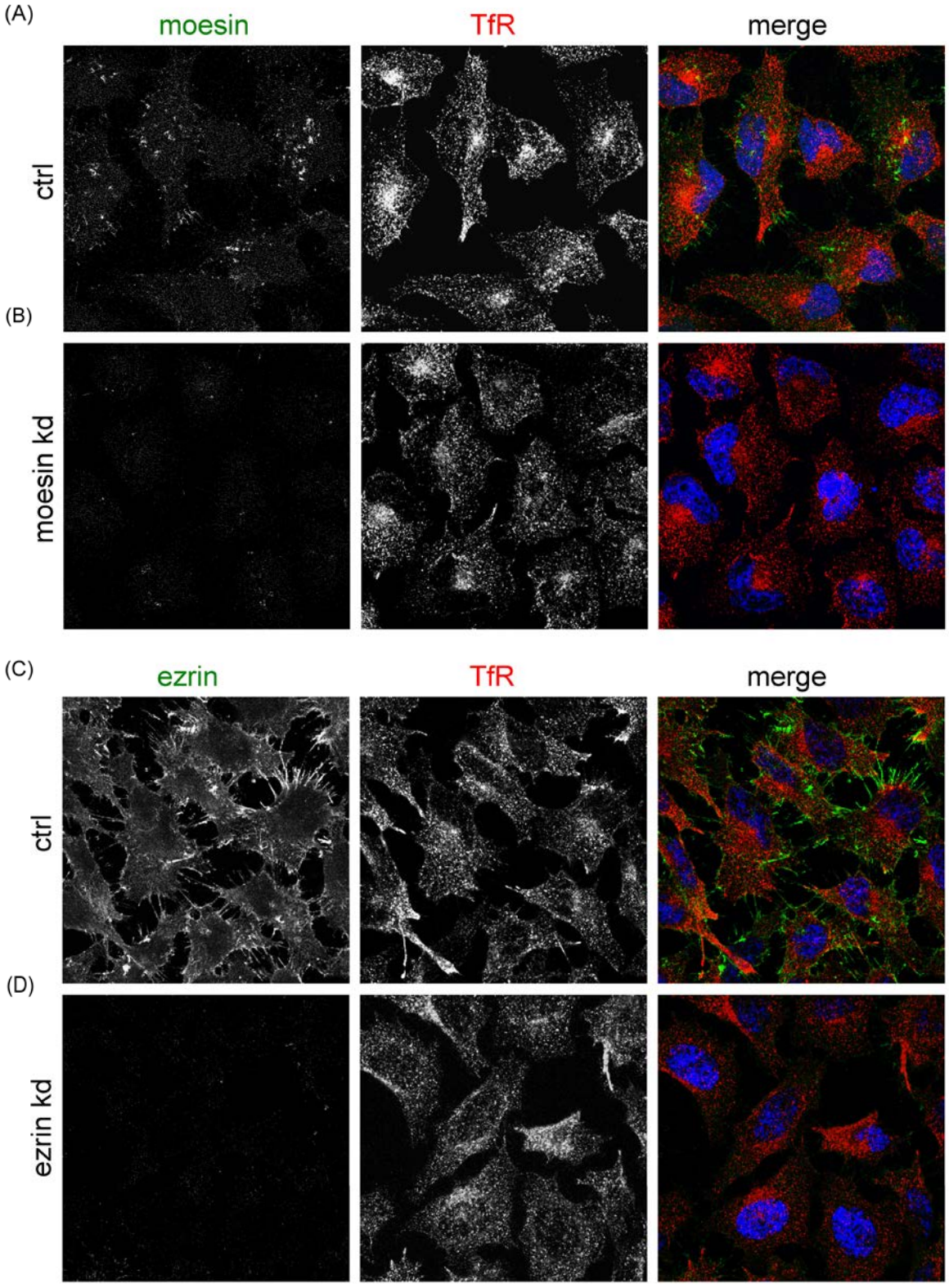

Figure 10 Microscopy study of TfR in ERM depleted HeLa cells. HeLa cells were stained for ezrin or moesin and TfR. The images are presented as two separate channels with the moesin, ezrin and TfR staining displayed in b/w, in addition to a colorized merged image including the DAPI staining (blue). (A) Moesin control cells (B) Moesin knockdown cells (C) Ezrin control cells (D) Ezrin knockdown cells.

3.6 High performance thin layer chromatography (HPTLC) of glycosphingolipids

To investigate whether the decrease in total cell associated Stx in response to ERM depletion was related to the level of the Stx glycosphingolipid receptor, various glycolipids were extracted and their level measured.

The glycosphingolipid globotriaocylceramide (Gb3) can act as receptor for Stx. Due to different headgroups, different glycosphingolipid classes can be separated by TLC. The class of Gb3 exists as different species, with hydrocarbon chains ranging from 16 carbon atoms to 24 carbon atoms. The different species within a class are only separated into two fractions termed C16 and C24. The C16 fraction consists mainly of C16:0 fatty acids, while the C24 fraction mainly consists of C22:0, C24:0 and C24:1. The level of Gb3 in HeLa cells in response to moesin siRNA depletion was assessed after lipid extraction from knockdown and control cells. The cells were centrifuged repeatedly after suspension in increasingly hydrophobic solvents (methanol:chloroform 1:0, 2:1, 1:1, 1:2, v/v) between each of the four centrifugation steps. The lipids contained in the combined methanol-chloroform fractions were then separated according to their hydrophobicity by thin layer chromatography on a HPTLC plate. The lipid bands were visualised by orcinol chemical staining and heating. The level of both Gb3 C16 and Gb3 C24 as well as the level of Gb4 C24, was reduced to ~ 70% after moesin knockdown (figure 11A). The endogenous level of Gb4 C16 was too low to be reliably quantified. Figure 11B shows a representative TLC plate with control cells compared to moesin knockdown cells (mo-1). Figure 11C shows a representative blot of the moesin level in the knockdown cells relative to the control cells. The moesin level was reduced to ~ 5% (mo-1). Interestingly, the level of Gb3 was reduced in response to moesin depletion.

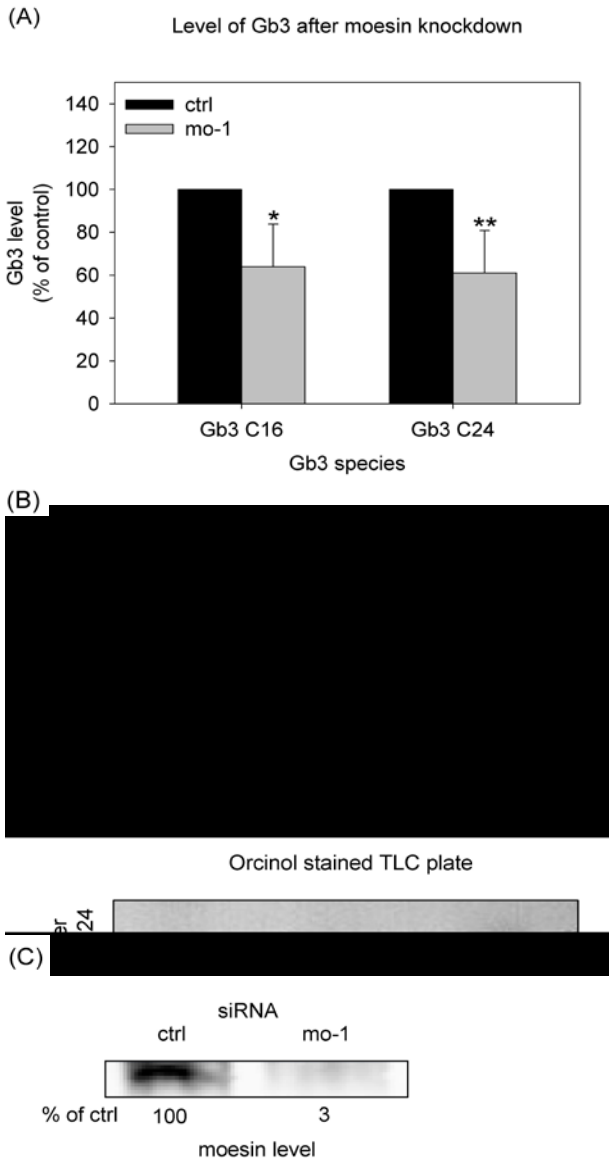

Figure 11 High performance thin layer chromatography (HPTLC) of glycosphingolipids in HeLa cells after moesin depletion. Lipids were extracted from siRNA treated HeLa cells and separated by HPTLC. (A) The total level of Gb3 C16 and Gb3 C24 in moesin knockdown cells relative to control cells (mean intensity ± S.D., $n \geq 4$. *; $p < 0.05$, **; $p < 0.005$). (B) A representative HPTLC plate after orcinol staining and heating. (C) Representative blot of the moesin level in the knockdown cells relative to control cells. The proteins were separated by SDS-PAGE and blotted to a PVDF membrane. The blot was stained with a primary ERM antibody and visualized by fluorescence. Only the moesin band is shown.

3.7 Microscopy study of the Gb3 level after moesin knockdown

Gb3 is known to be the main Stx receptor. To visualize the effect of moesin depletion on the Gb3 level in HeLa cells, live cells were stained with an anti-Gb3 antibody. Then the cells were fixed and permeabilized before they were stained with an anti-moesin antibody. The cells were then stained with fluorescently labelled secondary antibodies, with moesin in green and Gb3 in red, while the nucleus was stained with DAPI. As displayed in figure 12A and B, images were randomly taken of knockdown and control cells and the intensity of the Gb3 and the cytoplasmic moesin staining was

measured and analyzed. Figure 12C shows an intensity decrease of ~ 30% for the Gb3 staining and ~ 80% for the moesin staining in the moesin depleted cells compared to control. In agreement with the TLC experiments, moesin depletion significantly reduces the level of Gb3.

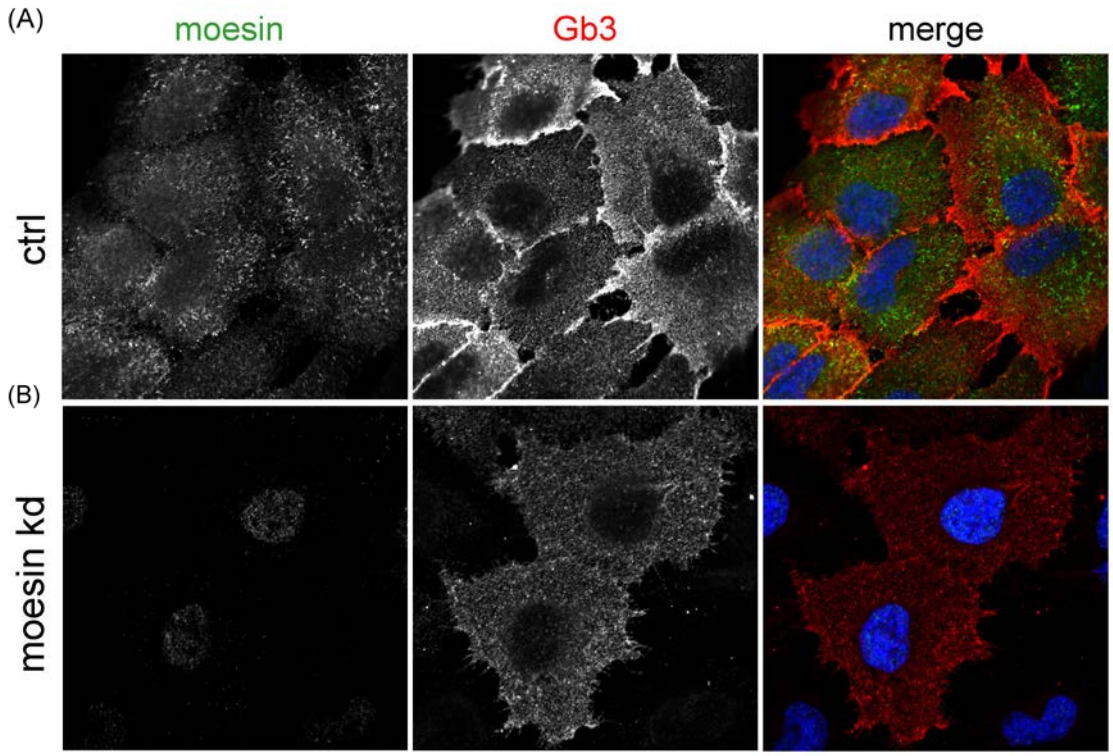

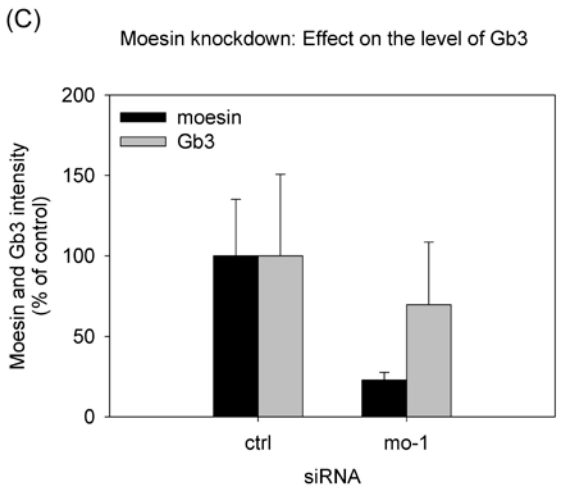

Figure 12 Microscopic analysis of the Gb3 level in HeLa cells after moesin knockdown. siRNA treated HeLa cells were stained for moesin and Gb3. The images are presented as two separate channels with the moesin and Gb3 staining displayed in b/w, in addition to a colorized merged image including the DAPI staining (blue). (A) Control cells. (B) Moesin knockdown cells. (C) Moesin and Gb3 intensity in moesin knockdown cells relative to control (mean intensity ± S.D., $n \geq 70$).

3.8 Transfection with siRNA resistant (siRNAr) ezrin and moesin genes in ERM depleted HeLa cells

To control that the phenotypic effects of ERM knockdown were in fact caused by lack of ERM function, ezrin and moesin depleted cells were transfected with ezrin and moesin siRNA resistant genes to try and reverse the knockdown effects. As previously mentioned, transfection with siRNA oligos induce degradation of mRNAs containing a specific nucleotide target sequence. Introducing siRNA resistant genes (siRNAr) with silent mutations in the target sequence results in translation of a functional protein (rescue). HeLa cells were transfected with the siRNA oligos mo-1 and ez-2. To restore their proteome, the cells were treated with vectors containing siRNAr genes encoding moesin or ezrin. In order to manipulate the cells to internalize the vectors, the siRNAr genes were transfected together with the FuGENE 6 transfection reagent. Knockdown cells were rescued with two different siRNAr-transfection reagent ratios in order to determine the optimal ratio for restoration of the endogenous protein levels. In figure 13A, knockdown cells were incubated with 1 µg siRNAr:6 µl FuGENE 6, restoring the ezrin level to ~ 90% of the endogenous level, while the moesin level was only restored to ~ 30%. In figure 13B, knockdown cells were incubated with 2 µg siRNAr:6 µl FuGENE 6, restoring the ezrin level to ~ 150% of the endogenous level, while the moesin level was restored to ~ 110%. In this initial experiment, the ezrin and moesin protein levels were restored to the physiological level. The cellular phenotypic response will be investigated in follow-up experiments.

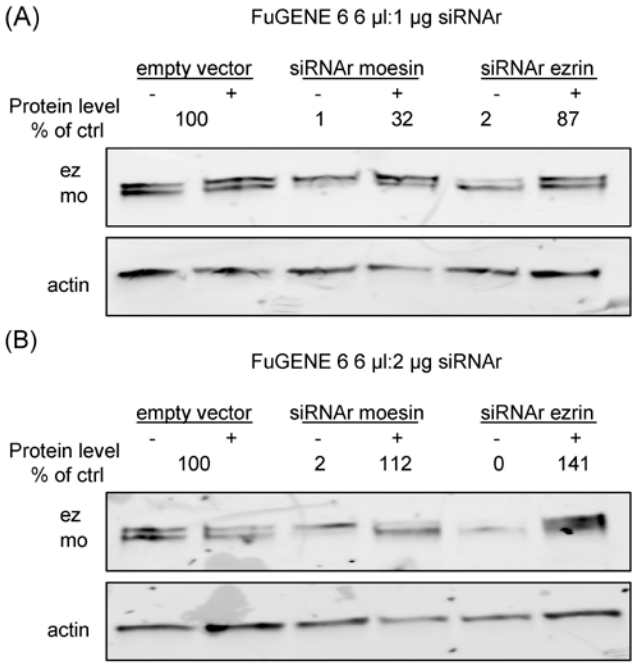

Figure 13 Rescue of moesin and ezrin in HeLa cells. siRNA treated HeLa cells were transfected with siRNAr moesin and ezrin DNA. (A) Western blot showing the ezrin (upper band), moesin (middle band) and actin (lower band) levels after rescue with 1 µg siRNAr: 6 µl FuGENE 6. The knockdown and rescue efficiencies are only calculated for the relevant protein (B). Western blot showing the ezrin, moesin and actin levels after rescue with 2 µg siRNAr:6 µl FuGENE 6 (as described in A). The blots were stained with primary antibodies targeting ERM proteins and actin. They were visualized by fluorescence.

3.9 The effect of Stx on ERM phosphorylation

As the role of the ERM proteins in binding and intracellular transport of Stx has been studied, it was relevant to investigate the effect of Stx incubation on the activation state of the ERM proteins in HeLa cells.

ERM proteins are known to exist either in a closed, inactive conformation in the cytoplasm or in an open, activated conformation at the plasma membrane and they have been shown to be activated by phosphorylation. To visualize the effect on the activation state of ERM proteins, HeLa cells were incubated with StxB for 10, 20 and 30 min. After fixation and permeabilization, the cells were stained with a phosphorylated ERM (pERM) antibody and a StxB antibody. The primary antibody staining was visualized by fluorescent secondary antibody treatment, with pERM in green and Stx in red, while the nucleus was stained with DAPI. Figure 14A and B displays HeLa cells incubated with StxB for 10 and 30 min, respectively. The StxB

subunit is known to accumulate in the TGN, as seen by the intense StxB staining near the nucleus after 30 min incubation. Intriguingly, there also seems to be a clear, time dependent decrease in phosphorylated ERM proteins after Stx incubation. However, these studies have to be considered preliminary as more conditions and time points should be tested. The intensity of the fluorescence at each time point is displayed in figure 14C.

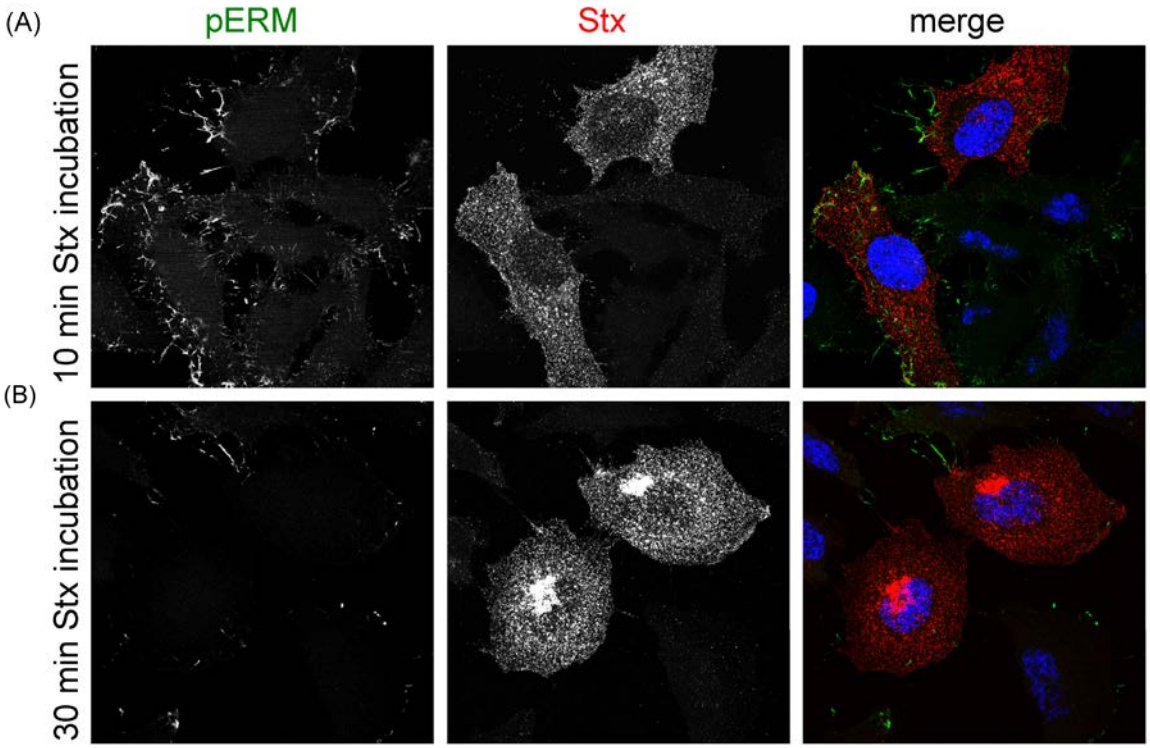

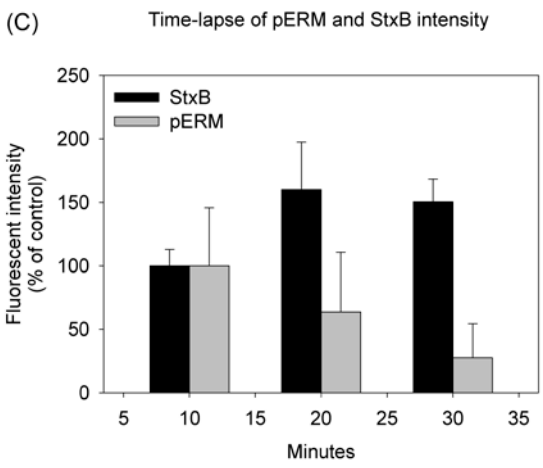

Figure 14 Microscopy study of the pERM level in HeLa cells in response to StxB incubation. HeLa cells were incubated with StxB for 10, 20 and 30 min and stained for pERM and StxB. The images are presented as two separate channels with the pERM and StxB staining displayed in b/w, in addition to a colorized merged image including the DAPI staining (blue). (A) Cells incubated with StxB for 10 min. (B) Cells incubated with StxB for 30 min. (C) The intensities of pERM in and StxB at different time points (mean intensities ± S.D., $n \geq 45$).

4. Discussion

In the present study, a new role for the ERM proteins in regulation of Gb3 expression at the cell surface is described. Intriguingly, ERM proteins function in the cytosol, while Gb3 is exclusively expressed in the non-cytosolic leaflet of membranes. These restrictions prohibit a direct interaction between Gb3 and the ERM proteins and potential, indirect regulatory mechanisms will therefore be discussed.

In order to study these mechanisms, HeLa cells were used as model cells. The HeLa cell line consists of carcinogenic cells derived from epithelial cells, and ezrin and moesin are regarded as the main ERM proteins expressed in these cells [10, 11]. This study is therefore focused on those two proteins. However, minor involvement by radixin cannot be excluded. A functional overlap between ezrin, radixin and moesin could therefore partially counteract the phenotypical effect caused by knockdown of ezrin and/or moesin. Additionally, new batches of HeLa cells were prepared in four week cycles and differences between batches as well as time-dependent changes in the batch might influence the cell tolerance for siRNA treatment. Besides, different siRNA oligos targeting the same proteins can cause different reductions in the protein levels (knockdown efficiency) and the cells might therefore display different phenotypic responses. Pairs of oligos were therefore applied in most of the experiments.

Stx is known to selectively bind the glycosphingolipid Gb3 and subsequently be endocytosed by clathrin-dependent endocytosis (CDE) [40] and clathrin-independent endocytosis (CIE) [90]. After endocytosis, Stx is transported retrogradely via early endosomes, the Golgi apparatus and the ER, before being translocated into the cytosol [41]. Gb3 has been shown to be important for the retrograde transport of Stx as well as its endocytosis [91]. The ERM proteins have been shown to be involved in intracellular trafficking mechanisms such as phagosomal fusion with lysosomes [92], receptor recycling [64, 65] and early to late endosomal transport [67]. In the present study, an effect of ERM depletion on transport of Stx to the Golgi apparatus and the ER was

demonstrated by sulfation and mannosylation experiments, respectively. This suggests that the ERM proteins might have a role in retrograde transport, but could also point towards a function in an upstream mechanism, such as binding and endocytosis of the toxin. The Stx transport to the Golgi seemed to be further reduced by double knockdown of moesin and ezrin (~ 90%), which might indicate a functional overlap for these proteins. However, it could also be a consequence of the lack of moesin or ezrin function in different preceding trafficking steps, giving a synergistic effect.

To investigate whether the reduced Stx transport to the Golgi and ER was caused by ERM absence at an upstream transport step, the effect on Stx binding and endocytosis in ERM depleted cells was examined by the Stx-biotin assay. The relative endocytosis was shown to be unaffected. However, the total amount of cell-associated Stx was reduced by ~ 35% (ez-1), ~ 55% (mo-1) and ~ 55% (ez-1/mo-1), and the results revealed a reduced amount of Stx associated with the cell surface. These results indicate that the ERM proteins are not directly involved in Stx endocytosis, but rather regulate membrane properties able to affect Stx binding. It has been reported that the ERM proteins associate with the cytosolic tails of several plasma membrane (PM) proteins (e.g. CD81 [78]), with membrane associated proteins (e.g. the raft resident EPB50 [80]) and with lipids (e.g. $PI(4,5)P_2$ [70]). These proteins and lipid are reported to serve as docking sites for ERM proteins and could mediate potential regulatory functions.

Ricin is known to bind all over the cell surface and subsequently be internalized by several mechanisms [41]. To clarify how widespread the functions of the ERM proteins are, ricin uptake and retrograde transport was also investigated. The amount of ricin reaching the Golgi network was not influenced by ERM depletion, indicating a specialized role for the ERM proteins. In order to further narrow the spectrum of possible ERM functions, the effect of ERM depletion on the level and distribution of a known CDE marker, the transferrin receptor (TfR), was investigated. Microscopy studies performed in the present work showed no effect neither on the TfR level nor on the TfR distribution after ERM knockdown, as earlier described for ezrin by Cao

et al [65] in another cell line. These results indicate that the ERM proteins might be selectively implicated in pathways other than the clathrin dependent pathway used by the transferrin receptor. There are however some reports about ERM involvement in clathrin-dependent processes, and moesin has been implicated in trafficking of clathrin coated vesicles [93].

Microscopy analysis of the effect of moesin knockdown on the Stx receptor Gb3 was conducted. A reduction in cell surface associated Gb3, as well as in total cell associated Gb3 was observed, a notion which was supported by TLC analysis. Both approaches showed a decrease of ~ 30% in the Gb3 level after moesin depletion. Gb3 has been shown to be concentrated in lipid rafts [90] and cluster upon Stx interaction [94]. Recent research suggests the existence of an intracellular Gb3 pool, enabling rapid replenishing of cell surface Gb3 levels, [95] and growing evidence situates rafts in internal membranes as well as on the PM [96]. Taken together, these results indicate a role for the ERM proteins in maintaining the normal level and distribution of Gb3 in a cell. As only the effect of moesin knockdown was investigated, a double knockdown of both ezrin and moesin could reveal a larger reduction in the level of Gb3.

There are at least three possible explanations for the fact that while total Gb3 levels were reduced by 30%, Stx binding was reduced by 55%. Firstly, it is simply possible that the amount of Gb3 at the cell surface is reduced to a larger extent than in the rest of the cell. Secondly, the Gb3 density in membrane rafts has been shown to be important for Stx binding [97]. This could mean that the cell surface level of Gb3 is specifically reduced in certain membrane areas in response to ERM depletion, causing decreased Gb3 density and availability in these areas. The Stx B-moiety is able to bind 15 Gb3 molecules [39]. The decreased Gb3 density might inhibit receptor clustering and result in Stx interacting with only a few Gb3 molecules, causing an insufficient Stx-Gb3 interaction for a stable binding to occur. Thereby, the sum of the decrease in the number of Gb3 molecules *per se*, as well as the effect of lower Gb3 density might give an amplified reduction in Stx binding in these areas. Thirdly, ERM knockdown might affect the receptor micro-environment which has been shown to be

important for Stx binding [53]. A combination of these effects is perhaps the most likely explanation.

The phosphatidylinositol-4-phosphate 5-kinases (PIP5KI) are found to accumulate in lipid rafts after activation of various membrane receptors [98]. Interestingly, PIP5KI phosphorylates PI(4)P to PI(4,5)P_2, which in turn is known to mediate activation of ERM proteins by inducing a conformational change [70]. In this study, a decrease in active, phosphorylated ERM (pERM) proteins from 10-30 min after Stx incubation was demonstrated. An initial rise in the pERM level in response to Stx binding has been shown in another cell line [99]. The decrease in the pERM level seen in the present work might be resulting from that the pERM levels has begun returning to the basal level by 10 min. However, these studies will be extended in future work.

Membrane rafts are enriched in glycosphingolipids and cholesterol [100] and rafts are also found in internal membranes [96]. Gb3 has been shown to be concentrated in lipid rafts, to cluster upon Stx interaction [90, 94] and to be important for Stx delivery to the Golgi apparatus and the ER [91]. The present study implicates ERM proteins in regulation of the Gb3 cell surface level. The ERM proteins are shown to be involved in phagosomal fusion with lysosomes [92], receptor recycling [64, 65] and early to late endosomal transport [67]. Additionally, absence of ezrin causes a shift in the transport of α1b-adrenergic receptor from recycling to lysosomal degradation [64]. Moreover, proteomic studies have placed moesin in membrane rafts [101, 102], and activated ERM proteins have been shown to recruit the Cdc42/Rho-specific guanine exchange factor (GEF) Dbl to the rafts [103]. Caveolin-1 is found to be a Cdc42 guanine nucleotide dissociation inhibitor (GDI) [104] and have been shown to bind a cross-linker at the acyl chain of [^{3}H]GM1(N_3), a derivative of the raft associated glycolipid GM1 [105]. This binding might imply a potential ability of caveolin-1 to bind lipids expressed in the outer PM monolayer. An interaction between ERM proteins, Dbl and caveolin-1 might initiate a positive feedback loop of ERM and Rho family GTPase activation, which could account for ERM knockdown effects on retrograde transport. Connecting actin to the membrane is a main structural feature of the ERM proteins [57] and actin

polymerization has been shown to be essential for e.g. raft dependent endocytic pathways and vesicle transport [106, 107]. Another central attribute of the ERM proteins is membrane polarization by actin reorganization, implicating the proteins in directed cell migration [9].

By interpreting my results in light of what is already known, I suggest that the ERM proteins function in a large protein complex involved in actin dependent sorting of endosomal vesicles containing glycosphingolipid enriched domains. Future studies to address the role of ERM proteins in trafficking of glycosphingolipids as well as Stx, would complement the emerging picture of the ERM protein functions both in normal cells and in cancer cells.

5. Reference list

1 Sandvig, K. *et al.* Retrograde transport of endocytosed Shiga toxin to the endoplasmic reticulum. *Nature* **358**, 510-512 (1992).

2 Sandvig, K. & van Deurs, B. Endocytosis, intracellular transport, and cytotoxic action of Shiga toxin and ricin. *Physiol Rev.* **76**, 949-966 (1996).

3 Smith, D. C. *et al.* Exogenous peptides delivered by ricin require processing by signal peptidase for transporter associated with antigen processing-independent MHC class I-restricted presentation. *J. Immunol.* **169**, 99-107 (2002).

4 Wiedlocha, A., Falnes, P. O., Madshus, I. H., Sandvig, K., & Olsnes, S. Dual mode of signal transduction by externally added acidic fibroblast growth factor. *Cell* **76**, 1039-1051 (1994).

5 Facchini, L. M. & Lingwood, C. A. A verotoxin 1 B subunit-lambda CRO chimeric protein specifically binds both DNA and globotriaosylceramide (Gb(3)) to effect nuclear targeting of exogenous DNA in Gb(3) positive cells. *Exp. Cell Res.* **269**, 117-129 (2001).

6 Meng, J. & Doyle, M. P. Emerging issues in microbiological food safety. *Annu. Rev. Nutr.* **17**, 255-275 (1997).

7 Knight, B. Ricin--a potent homicidal poison. *Br. Med. J.* **1**, 350-351 (1979).

8 McClatchey, A. I. & Fehon, R. G. Merlin and the ERM proteins--regulators of receptor distribution and signaling at the cell cortex. *Trends Cell Biol.* **19**, 198-206 (2009).

9 Bretscher, A., Edwards, K., & Fehon, R. G. ERM proteins and merlin: integrators at the cell cortex. *Nat. Rev. Mol. Cell Biol.* **3**, 586-599 (2002).

10 Maeda, M., Matsui, T., Imamura, M., Tsukita, S., & Tsukita, S. Expression level, subcellular distribution and rho-GDI binding affinity of merlin in comparison with Ezrin/Radixin/Moesin proteins. *Oncogene* **18**, 4788-4797 (1999).

11 Shcherbina, A., Bretscher, A., Kenney, D. M., & Remold-O'Donnell, E. Moesin, the major ERM protein of lymphocytes and platelets, differs from ezrin in its insensitivity to calpain. *fl* **443**, 31-36 (1999).

12 Wadsworth, A. B. Studies on pneumococcus infection in animals: First paper. *J. Exp. Med.* **16**, 54-77 (1912).

13 Mayor, S. & Pagano, R. E. Pathways of clathrin-independent endocytosis. *Nat. Rev. Mol. Cell Biol.* **8**, 603-612 (2007).

14 Pearse, B. M. Clathrin: a unique protein associated with intracellular transfer of membrane by coated vesicles. *Proc. Natl. Acad. Sci. U. S. A* **73**, 1255-1259 (1976).

15 Pearse, B. M., Smith, C. J., & Owen, D. J. Clathrin coat construction in endocytosis. *Curr. Opin. Struct. Biol.* **10**, 220-228 (2000).

16 Damke, H., Baba, T., van der Bliek, A. M., & Schmid, S. L. Clathrin-independent pinocytosis is induced in cells overexpressing a temperature-sensitive mutant of dynamin. *J. Cell Biol.* **131**, 69-80 (1995).

17 Ellis, S. & Mellor, H. Regulation of endocytic traffic by rho family GTPases. *Trends Cell Biol.* **10**, 85-88 (2000).

18 Moss, J. & Vaughan, M. Structure and function of ARF proteins: activators of cholera toxin and critical components of intracellular vesicular transport processes. *J. Biol. Chem.* **270**, 12327-12330 (1995).

19 Ait-Slimane, T., Galmes, R., Trugnan, G., & Maurice, M. Basolateral internalization of GPI-anchored proteins occurs via a clathrin-independent flotillin-dependent pathway in polarized hepatic cells. *Mol. Biol. Cell* **20**, 3792-3800 (2009).

20 Frick, M. *et al.* Coassembly of flotillins induces formation of membrane microdomains, membrane curvature, and vesicle budding. *Curr. Biol.* **17**, 1151-1156 (2007).

21 Parton, R. G. Caveolae--from ultrastructure to molecular mechanisms. *Nat. Rev. Mol. Cell Biol.* **4**, 162-167 (2003).

22 Hill, M. M. *et al.* PTRF-Cavin, a conserved cytoplasmic protein required for caveola formation and function. *Cell* **132**, 113-124 (2008).

23 Parton, R. G. & Howes, M. T. Revisiting caveolin trafficking: the end of the caveosome. *J. Cell Biol.* **191**, 439-441 (2010).

24 Tagawa, A. *et al.* Assembly and trafficking of caveolar domains in the cell: caveolae as stable, cargo-triggered, vesicular transporters. *J. Cell Biol.* **170**, 769-779 (2005).

25 Parton, R. G. & Richards, A. A. Lipid rafts and caveolae as portals for endocytosis: new insights and common mechanisms. *Traffic.* **4**, 724-738 (2003).

26 Pelkmans, L., Burli, T., Zerial, M., & Helenius, A. Caveolin-stabilized membrane domains as multifunctional transport and sorting devices in endocytic membrane traffic. *Cell* **118**, 767-780 (2004).

27 Octave, J. N., Schneider, Y. J., Crichton, R. R., & Trouet, A. Transferrin uptake by cultured rat embryo fibroblasts. The influence of temperature and incubation time, subcellular distribution and short-term kinetic studies. *Eur. J. Biochem.* **115**, 611-618 (1981).

28 Bleil, J. D. & Bretscher, M. S. Transferrin receptor and its recycling in HeLa cells. *EMBO J.* **1**, 351-355 (1982).

29 Park, S. W., Moon, Y. A., & Horton, J. D. Post-transcriptional regulation of low density lipoprotein receptor protein by proprotein convertase subtilisin/kexin type 9a in mouse liver. *J. Biol. Chem.* **279**, 50630-50638 (2004).

30 Johnson, L. S., Dunn, K. W., Pytowski, B., & McGraw, T. E. Endosome acidification and receptor trafficking: bafilomycin A1 slows receptor externalization by a mechanism involving the receptor's internalization motif. *Mol. Biol. Cell* **4**, 1251-1266 (1993).

31 Sorkin, A. & Duex, J. E. Quantitative analysis of endocytosis and turnover of epidermal growth factor (EGF) and EGF receptor. *Curr. Protoc. Cell Biol.* **15**, Unit (2010).

32 Steinman, R. M., Mellman, I. S., Muller, W. A., & Cohn, Z. A. Endocytosis and the recycling of plasma membrane. *J. Cell Biol.* **96**, 1-27 (1983).

33 Rohn, J. L. & Baum, B. Actin and cellular architecture at a glance. *J. Cell Sci.* **123**, 155-158 (2010).

34 Liu, J., Kaksonen, M., Drubin, D. G., & Oster, G. Endocytic vesicle scission by lipid phase boundary forces. *Proc. Natl. Acad. Sci. U. S. A* **103**, 10277-10282 (2006).

35 Kaksonen, M., Sun, Y., & Drubin, D. G. A pathway for association of receptors, adaptors, and actin during endocytic internalization. *Cell* **115**, 475-487 (2003).

36 Sandvig, K., Torgersen, M. L., Engedal, N., Skotland, T., & Iversen, T. G. Protein toxins from plants and bacteria: probes for intracellular transport and tools in medicine. *fl* **584**, 2626-2634 (2010).

37 Palermo, M. S., Exeni, R. A., & Fernandez, G. C. Hemolytic uremic syndrome: pathogenesis and update of interventions. *Expert. Rev. Anti. Infect. Ther.* **7**, 697-707 (2009).

38 Sehgal, P., Khan, M., Kumar, O., & Vijayaraghavan, R. Purification, characterization and toxicity profile of ricin isoforms from castor beans. *Food Chem. Toxicol.* **48**, 3171-3176 (2010).

39 Ling, H. *et al.* Structure of the shiga-like toxin I B-pentamer complexed with an analogue of its receptor Gb3. *Biochemistry* **37**, 1777-1788 (1998).

40 Lauvrak, S. U., Torgersen, M. L., & Sandvig, K. Efficient endosome-to-Golgi transport of Shiga toxin is dependent on dynamin and clathrin. *J. Cell Sci.* **117**, 2321-2331 (2004).

41 Sandvig, K. & van Deurs, B. Delivery into cells: lessons learned from plant and bacterial toxins. *Gene Ther.* **12**, 865-872 (2005).

42 Sandvig, K. & van Deurs, B. Endocytosis without clathrin. *Trends Cell Biol.* **4**, 275-277 (1994).

43 Raa, H. *et al.* Glycosphingolipid requirements for endosome-to-Golgi transport of Shiga toxin. *Traffic.* **10**, 868-882 (2009).

44 Bujny, M. V., Popoff, V., Johannes, L., & Cullen, P. J. The retromer component sorting nexin-1 is required for efficient retrograde transport of Shiga toxin from early endosome to the trans Golgi network. *J. Cell Sci.* **120**, 2010-2021 (2007).

45 Dyve, A. B., Bergan, J., Utskarpen, A., & Sandvig, K. Sorting nexin 8 regulates endosome-to-Golgi transport. *Biochem. Biophys. Res. Commun.* **390**, 109-114 (2009).

46 Girod, A. *et al.* Evidence for a COP-I-independent transport route from the Golgi complex to the endoplasmic reticulum. *Nat. Cell Biol.* **1**, 423-430 (1999).

47 Sandvig, K., Bergan, J., Dyve, A. B., Skotland, T., & Torgersen, M. L. Endocytosis and retrograde transport of Shiga toxin. *Toxicon*(2009).

48 Yu, M. & Haslam, D. B. Shiga toxin is transported from the endoplasmic reticulum following interaction with the luminal chaperone HEDJ/ERdj3. *Infect. Immun.* **73**, 2524-2532 (2005).

49 Zumbrun, S. D. *et al.* Human intestinal tissue and cultured colonic cells contain globotriaosylceramide synthase mRNA and the alternate Shiga toxin receptor globotetraosylceramide. *Infect. Immun.* **78**, 4488-4499 (2010).

50 Lingwood, C. A., Khine, A. A., & Arab, S. Globotriaosyl ceramide (Gb3) expression in human tumour cells: intracellular trafficking defines a new retrograde transport pathway from the cell surface to the nucleus, which correlates with sensitivity to verotoxin. *Acta Biochim. Pol.* **45**, 351-359 (1998).

51 El Alaoui, A. *et al.* Shiga toxin-mediated retrograde delivery of a topoisomerase I inhibitor prodrug. *Angew. Chem. Int. Ed Engl.* **46**, 6469-6472 (2007).

52 Lingwood, C. A., Binnington, B., Manis, A., & Branch, D. R. Globotriaosyl ceramide receptor function - where membrane structure and pathology intersect. *FEBS Lett.* **584**, 1879-1886 (2010).

53 Lingwood, C. A. *et al.* New aspects of the regulation of glycosphingolipid receptor function. *Chemistry and Physics of Lipids* **163**, 27-35 (2010).

54 Fehon, R. G., McClatchey, A. I., & Bretscher, A. Organizing the cell cortex: the role of ERM proteins. *Nat. Rev. Mol. Cell Biol.* **11**, 276-287 (2010).

55 Berryman, M., Franck, Z., & Bretscher, A. Ezrin is concentrated in the apical microvilli of a wide variety of epithelial cells whereas moesin is found primarily in endothelial cells. *J. Cell Sci.* **105**, 1025-1043 (1993).

56 Amieva, M. R., Wilgenbus, K. K., & Furthmayr, H. Radixin is a component of hepatocyte microvilli in situ. *Exp. Cell Res.* **210**, 140-144 (1994).

57 Takeuchi, K. *et al.* Perturbation of cell adhesion and microvilli formation by antisense oligonucleotides to ERM family members. *J. Cell Biol.* **125**, 1371-1384 (1994).

58 Yonemura, S., Matsui, T., Tsukita, S., & Tsukita, S. Rho-dependent and -independent activation mechanisms of ezrin/radixin/moesin proteins: an essential role for polyphosphoinositides in vivo. *J. Cell Sci.* **115**, 2569-2580 (2002).

59 Gautreau, A., Louvard, D., & Arpin, M. Morphogenic effects of ezrin require a phosphorylation-induced transition from oligomers to monomers at the plasma membrane. *J. Cell Biol.* **150**, 193-203 (2000).

60 Berryman, M., Gary, R., & Bretscher, A. Ezrin oligomers are major cytoskeletal components of placental microvilli: a proposal for their involvement in cortical morphogenesis. *J. Cell Biol.* **131**, 1231-1242 (1995).

61 Doi, Y. *et al.* Normal development of mice and unimpaired cell adhesion/cell motility/actin-based cytoskeleton without compensatory up-regulation of ezrin or radixin in moesin gene knockout. *J. Biol. Chem.* **274**, 2315-2321 (1999).

62 Kikuchi, S. *et al.* Radixin deficiency causes conjugated hyperbilirubinemia with loss of Mrp2 from bile canalicular membranes. *Nat. Genet.* **31**, 320-325 (2002).

63 Shaffer, M. H. *et al.* Ezrin is highly expressed in early thymocytes, but dispensable for T cell development in mice. *PLoS. One.* **5**, e12404 (2010).

64 Stanasila, L., Abuin, L., Diviani, D., & Cotecchia, S. Ezrin directly interacts with the alpha1b-adrenergic receptor and plays a role in receptor recycling. *J. Biol. Chem.* **281**, 4354-4363 (2006).

65 Cao, T. T., Deacon, H. W., Reczek, D., Bretscher, A., & von Zastrow, M. A kinase-regulated PDZ-domain interaction controls endocytic sorting of the beta2-adrenergic receptor. *Nature* **401**, 286-290 (1999).

66 Harder, T., Kellner, R., Parton, R. G., & Gruenberg, J. Specific release of membrane-bound annexin II and cortical cytoskeletal elements by sequestration of membrane cholesterol. *Mol. Biol. Cell* **8**, 533-545 (1997).

67 Chirivino, D. *et al.* The ERM proteins interact with the class C-Vps/HOPS complex to regulate the maturation of endosomes. *Mol. Biol. Cell*(2010).

68 Gusella, J. F., Ramesh, V., MacCollin, M., & Jacoby, L. B. Neurofibromatosis 2: loss of merlin's protective spell. *Curr. Opin. Genet. Dev.* **6**, 87-92 (1996).

69 McClatchey, A. I., Saotome, I., Ramesh, V., Gusella, J. F., & Jacks, T. The Nf2 tumor suppressor gene product is essential for extraembryonic development immediately prior to gastrulation. *Genes Dev.* **11**, 1253-1265 (1997).

70 Fievet, B. T. *et al.* Phosphoinositide binding and phosphorylation act sequentially in the activation mechanism of ezrin. *J. Cell Biol.* **164**, 653-659 (2004).

71 Matsui, T. *et al.* Rho-kinase phosphorylates COOH-terminal threonines of ezrin/radixin/moesin (ERM) proteins and regulates their head-to-tail association. *J. Cell Biol.* **140**, 647-657 (1998).

72 Ng, T. *et al.* Ezrin is a downstream effector of trafficking PKC-integrin complexes involved in the control of cell motility. *EMBO J.* **20**, 2723-2741 (2001).

73 Simons, P. C., Pietromonaco, S. F., Reczek, D., Bretscher, A., & Elias, L. C-terminal threonine phosphorylation activates ERM proteins to link the cell's cortical lipid bilayer to the cytoskeleton. *Biochem. Biophys. Res. Commun.* **253**, 561-565 (1998).

74 Nakamura, N. *et al.* Phosphorylation of ERM proteins at filopodia induced by Cdc42. *Genes Cells* **5**, 571-581 (2000).

75 Roch, F. *et al.* Differential roles of PtdIns(4,5)P2 and phosphorylation in moesin activation during Drosophila development. *J. Cell Sci.* **123**, 2058-2067 (2010).

76 Krieg, J. & Hunter, T. Identification of the two major epidermal growth factor-induced tyrosine phosphorylation sites in the microvillar core protein ezrin. *J. Biol. Chem.* **267**, 19258-19265 (1992).

77 Crepaldi, T., Gautreau, A., Comoglio, P. M., Louvard, D., & Arpin, M. Ezrin is an effector of hepatocyte growth factor-mediated migration and morphogenesis in epithelial cells. *J. Cell Biol.* **138**, 423-434 (1997).

78 Coffey, G. P. *et al.* Engagement of CD81 induces ezrin tyrosine phosphorylation and its cellular redistribution with filamentous actin. *J. Cell Sci.* **122**, 3137-3144 (2009).

79 Garbett, D., Lalonde, D. P., & Bretscher, A. The scaffolding protein EBP50 regulates microvillar assembly in a phosphorylation-dependent manner. *J. Cell Biol.*(2010).

80 Ruppelt, A. *et al.* Inhibition of T cell activation by cyclic adenosine 5'-monophosphate requires lipid raft targeting of protein kinase A type I by the A-kinase anchoring protein ezrin. *J. Immunol.* **179**, 5159-5168 (2007).

81 Yonemura, S. *et al.* Ezrin/radixin/moesin (ERM) proteins bind to a positively charged amino acid cluster in the juxta-membrane cytoplasmic domain of CD44, CD43, and ICAM-2. *J. Cell Biol.* **140**, 885-895 (1998).

82 Trofatter, J. A. *et al.* A novel moesin-, ezrin-, radixin-like gene is a candidate for the neurofibromatosis 2 tumor suppressor. *Cell* **75**, 826 (1993).

83 McClatchey, A. I. Merlin and ERM proteins: unappreciated roles in cancer development? *Nat. Rev. Cancer* **3**, 877-883 (2003).

84 Tran, Q. C., Gautreau, A., Arpin, M., & Treisman, R. Ezrin function is required for ROCK-mediated fibroblast transformation by the Net and Dbl oncogenes. *EMBO J.* **19**, 4565-4576 (2000).

85 Wick, W. *et al.* Ezrin-dependent promotion of glioma cell clonogenicity, motility, and invasion mediated by BCL-2 and transforming growth factor-beta2. *J. Neurosci.* **21**, 3360-3368 (2001).

86 Akisawa, N., Nishimori, I., Iwamura, T., Onishi, S., & Hollingsworth, M. A. High levels of ezrin expressed by human pancreatic adenocarcinoma cell lines with high metastatic potential. *Biochem. Biophys. Res. Commun.* **258**, 395-400 (1999).

87 Nestl, A. *et al.* Gene expression patterns associated with the metastatic phenotype in rodent and human tumors. *Cancer Res.* **61**, 1569-1577 (2001).

88 Khanna, C. *et al.* Metastasis-associated differences in gene expression in a murine model of osteosarcoma. *Cancer Res.* **61**, 3750-3759 (2001).

89 Speck, O., Hughes, S. C., Noren, N. K., Kulikauskas, R. M., & Fehon, R. G. Moesin functions antagonistically to the Rho pathway to maintain epithelial integrity. *Nature* **421**, 83-87 (2003).

90 Betz, J. *et al.* Shiga toxin glycosphingolipid receptors in microvascular and macrovascular endothelial cells: association with membrane lipid raft microdomains that differ by their stability to cholesterol depletion. *J. Lipid Res.*(2011).

91 Falguieres, T. *et al.* Targeting of Shiga toxin B-subunit to retrograde transport route in association with detergent-resistant membranes. *Mol. Biol. Cell* **12**, 2453-2468 (2001).

92 Marion, S. *et al.* Ezrin promotes actin assembly at the phagosome membrane and regulates phago-lysosomal fusion. *Traffic.*(2011).

93 Barroso-Gonzalez, J., Machado, J. D., Garcia-Exposito, L., & Valenzuela-Fernandez, A. Moesin regulates the trafficking of nascent clathrin-coated vesicles. *J. Biol. Chem.* **284**, 2419-2434 (2009).

94 Kovbasnjuk, O., Edidin, M., & Donowitz, M. Role of lipid rafts in Shiga toxin 1 interaction with the apical surface of Caco-2 cells. *J. Cell Sci.* **114**, 4025-4031 (2001).

95 Falguieres, T. *et al.* Functionally different pools of Shiga toxin receptor, globotriaosyl ceramide, in HeLa cells. *FEBS J.* **273**, 5205-5218 (2006).

96 Kruth, H. S. *et al.* Monoclonal antibody detection of plasma membrane cholesterol microdomains responsive to cholesterol trafficking. *J. Lipid Res.* **42**, 1492-1500 (2001).

97 Hanashima, T. *et al.* Effect of Gb3 in lipid rafts in resistance to Shiga-like toxin of mutant Vero cells. *Microb. Pathog.* **45**, 124-133 (2008).

98 Kwiatkowska, K. One lipid, multiple functions: how various pools of PI(4,5)P(2) are created in the plasma membrane. *Cell Mol. Life Sci.* **67**, 3927-3946 (2010).

99 Takenouchi, H. *et al.* Shiga toxin binding to globotriaosyl ceramide induces intracellular signals that mediate cytoskeleton remodeling in human renal carcinoma-derived cells. *J. Cell Sci.* **117**, 3911-3922 (2004).

100 Parton, R. G. Caveolae and caveolins. *Curr. Opin. Cell Biol.* **8**, 542-548 (1996).

101 Li, N. *et al.* Monocyte lipid rafts contain proteins implicated in vesicular trafficking and phagosome formation. *Proteomics.* **3**, 536-548 (2003).

102 Foster, L. J., de Hoog, C. L., & Mann, M. Unbiased quantitative proteomics of lipid rafts reveals high specificity for signaling factors. *Proc. Natl. Acad. Sci. U. S. A* **100**, 5813-5818 (2003).

103 Prag, S. *et al.* Activated ezrin promotes cell migration through recruitment of the GEF Dbl to lipid rafts and preferential downstream activation of Cdc42. *Mol. Biol. Cell* **18**, 2935-2948 (2007).

104 Nevins, A. K. & Thurmond, D. C. Caveolin-1 functions as a novel Cdc42 guanine nucleotide dissociation inhibitor in pancreatic beta-cells. *J. Biol. Chem.* **281**, 18961-18972 (2006).

105 Fra, A. M., Masserini, M., Palestini, P., Sonnino, S., & Simons, K. A photo-reactive derivative of ganglioside GM1 specifically cross-links VIP21-caveolin on the cell surface. *FEBS Lett.* **375**, 11-14 (1995).

106 Parton, R. G., Joggerst, B., & Simons, K. Regulated internalization of caveolae. *J. Cell Biol.* **127**, 1199-1215 (1994).

107 Pelkmans, L., Puntener, D., & Helenius, A. Local actin polymerization and dynamin recruitment in SV40-induced internalization of caveolae. *Science* **296**, 535-539 (2002).